

Novel Regulators of Planar Cell Polarity: A Genetic Analysis in *Drosophila*

Ursula Weber, William J. Gault,¹ Patricio Olguin, Ekaterina Serysheva, and Marek Mlodzik²
 Department of Developmental and Regenerative Biology, Mount Sinai School of Medicine, New York, New York 10029

ABSTRACT Planar cell polarity (PCP) is a common feature of many epithelia and epithelial organs. Although progress has been made in the dissection of molecular mechanisms regulating PCP, many questions remain. Here we describe a screen to identify novel PCP regulators in *Drosophila*. We employed mild gain-of-function (GOF) phenotypes of two cytoplasmic Frizzled (Fz)/PCP core components, Diego (Dgo) and Prickle (Pk), and screened these against the DrosDel genome-wide deficiency collection for dominant modifiers. Positive genomic regions were rescreened and narrowed down with smaller overlapping deficiencies from the Exelixis collection and RNAi-mediated knockdown applied to individual genes. This approach isolated new regulators of PCP, which were confirmed with loss-of-function analyses displaying PCP defects in the eye and/or wing. Furthermore, knockdown of a subset was also sensitive to *dgo* dosage or dominantly modified a *dishevelled* (*dsh*) GOF phenotype, supporting a role in Fz/PCP-mediated polarity establishment. Among the new “PCP” genes we identified several kinases, enzymes required for lipid modification, scaffolding proteins, and genes involved in substrate modification and/or degradation. Interestingly, one of them is a member of the Meckel-Gruber syndrome factors, associated with human ciliopathies, suggesting an important role for cell polarity in nonciliated cells.

PLANAR cell polarity (PCP) controls the orientation of single cells or groups of cells within a plane of tissue and is conserved throughout the animal kingdom (Seifert and Mlodzik 2007; Wang and Nathans 2007; Bayly and Axelrod 2011). In *Drosophila*, for example, PCP manifests in each wing cell as a single distally pointing hair, or in the compound eye in the arrangement of photoreceptor cells (Adler 2002; Strutt 2003; Klein and Mlodzik 2005; Seifert and Mlodzik 2007). When PCP establishment is perturbed in the wing, hairs can point in random directions and/or several wing hairs form in single cells. In the eye, PCP controls two aspects of ommatidial orientation: photoreceptor R3 and R4 cell fate determination and a subsequent 90° rotation of an entire ommatidium, which together establish a mirror image symmetry along the dorsoventral boundary, the equator (Mlodzik 1999; Strutt and Strutt 1999). In this

context, PCP defects can produce random chiral arrangements of photoreceptors and symmetrical and misrotated ommatidia (Adler 2002; Strutt 2003; Klein and Mlodzik 2005; Seifert and Mlodzik 2007).

A conserved core set of proteins is critical for PCP establishment. These include the multipass *trans*-membrane proteins Frizzled (Fz), Strabismus/Van Gogh (Stbm/Vang), and Flamingo/Starry night (Fmi/Stn, an atypical cadherin), and the cytoplasmic factors Dishevelled (Dsh), Prickle (Pk), and Diego (Dgo) (Adler 2002; Strutt 2003; Klein and Mlodzik 2005; Seifert and Mlodzik 2007; Wang and Nathans 2007; Bayly and Axelrod 2011). The Fz receptor recruits and signals through Dsh, a component shared with the canonical *wingless* (*wg*)/Wnt signaling pathway (Boutros and Mlodzik 1999; Wallingford and Habas 2005). The other core PCP factors are thought to regulate Fz/Dsh activity and/or localization: Dgo promotes Fz/Dsh complex formation, whereas Stbm/Vang and Pk antagonize it (Tree *et al.* 2002; Jenny *et al.* 2005); Fmi/Stn is thought to promote the function of both complexes by stabilizing their membrane association (Sahai *et al.* 1998; Usui *et al.* 1999; Das *et al.* 2002; Lawrence *et al.* 2004; Klein and Mlodzik 2005; Casal *et al.* 2006; Chen *et al.* 2008; Strutt and Strutt 2008, 2009). As a result of their interactions, the core components localize asymmetrically in *Drosophila*

Copyright © 2012 by the Genetics Society of America
 doi: 10.1534/genetics.111.137190

Manuscript received November 25, 2011; accepted for publication February 22, 2012
 Supporting information is available online at <http://www.genetics.org/content/suppl/2012/03/05/genetics.111.137190.DC1>.

¹Present address: Memorial Sloan-Kettering Institute, 1275 York Ave., New York, NY 10065.

²Corresponding author: Department of Developmental and Regenerative Biology, Mount Sinai School of Medicine, 1 Gustave L. Levy Place, New York, NY 10029.
 E-mail: marek.mlodzik@mssm.edu

tissues, forming two complexes on opposite sides of any given cell. In the wing, *Stbm/Vang* and *Pk* accumulate in complexes on the proximal side of each cell, whereas *Fz*, *Dsh*, and *Dgo* form a complex that localizes distally. *Fmi/Stan* is part of both complexes (Lawrence *et al.* 2004; Klein and Mlodzik 2005; Casal *et al.* 2006; Chen *et al.* 2008; Strutt and Strutt 2009). Whereas the interactions among the core factors are beginning to be understood, less is known about potential upstream long-range signaling input (Wu and Mlodzik 2009) or downstream cellular interactions/effectors of the complexes.

Besides the *Fz/PCP* core group, a parallel pathway anchored around the protocadherins *Fat* (*Ft*) and *Dachsous* (*Ds*) also acts in *PCP* establishment (Casal *et al.* 2006; Lawrence *et al.* 2007). In certain contexts *Fat/Ds* and *Fz/PCP* signaling act redundantly, though the exact relationship between these pathways remains unclear (Casal *et al.* 2006; Donoughe and Dinardo 2011). Similarly, although apical-basal (*A/B*)-polarity determinants can interact with *Fz/PCP* factors (Djiane *et al.* 2005; Courbard *et al.* 2009) and *A/B* polarity in epithelia is generally a prerequisite for *PCP*-type polarity, interactions among *A/B*-polarity factors and *PCP* core components are not well defined.

To gain insight into the regulatory interactions among the core *Fz/PCP* genes, their relationship with other polarity determinants, and to identify novel effectors of the core *PCP* complexes, we designed a genetic screen employing mild core *PCP* factor overexpression. We selected *Pk* and *Dgo*, because they act at the level of *Dsh*, compete for *Dsh* binding *in vitro*, and antagonize each other in the context of *PCP* establishment (Jenny *et al.* 2005). Gain-of-function (*GOF*) backgrounds of *Dgo* and *Pk* were used in a genome-wide modifier screen to select for genetic interactions with both complexes. Furthermore, we took advantage of several recently available genetic tools in *Drosophila*: collections of overlapping deficiencies generated by recombinant techniques in genetically identical animals, including the *DrosDel* (Ryder *et al.* 2007) and *Exelixis* (Parks *et al.* 2004) deficiency collections, as well as transgenic *RNAi* tools available for most genes [Vienna *Drosophila* *RNAi* Collection (VDRC), Dietzl *et al.* 2007, and Nippon Institute of Genetics (NIG)]. This was combined with *in vivo* imaging of GFP-labeled rhabdomeres (animals carried a *rhodopsin1-GFP* transgene, referred to as *Rh1-GFP*; Pichaud and Desplan 2001) allowing for rapid verification of modifiers of the core *PCP* phenotypes.

In this study, we isolated several new regulators of *PCP* that either enhanced or suppressed the *pk* or *dgo* *GOF* phenotype in the adult eye and/or wing. Of the 195 deficiencies initially screened, 11 were confirmed by smaller deficiencies, *RNAi* knockdowns, and/or mutant alleles. Two deficiencies harbored *dachsous* (*ds*) and *Delta* (*DI*), which are known *PCP* factors acting in the parallel *Fat/Ds* pathway or as an eye-specific effector of *Fz/PCP* signaling, respectively. The new *PCP* regulators include kinases, scaffolding proteins, lipid modification enzymes, and factors involved in covalent protein modification and degradation. Loss-of-function

analyses of many of these genes indicated that they indeed function in *PCP* establishment in the eye and/or wing. Furthermore, knockdown of a subset of these genes was shown to be sensitive to *dgo* dosage or could dominantly modify *dsh* *GOF* phenotypes, supporting a role in *PCP* establishment.

Materials and Methods

Fly stocks and genetic screen

Recombinants of *Rh1-GFP*, *sev-GAL4*, and *UAS-dgo* or *UAS-pk^{sple}* (the *Sple* isoform of *Pk* (Gubb *et al.* 1999; Jenny *et al.* 2005) (referred to as *sev-GAL4*, *UAS-dgo*, or *sev-GAL4*, *UAS-pk*, respectively) were established and tested for reproducible chirality and ommatidial rotation defects. Testcrosses to *pk¹³* and *pk^{sple1}* alleles revealed that the *w*; *UAS-dgo*, *Rh1-GFP*; *sev-GAL4* recombinant flies carry a strong *pk* (*pk-sple*) mutation, originating from the *Rh1-GFP* chromosome, affecting all adult tissues. The *sev-GAL4* driver (expressed during *PCP* establishment in a subset of R cells including the R3/R4 precursors) has basal expression in other tissues due to the presence of a heat-shock promoter (from *hsp70*). *sev-GAL4* expression of *PCP* proteins has been observed to induce wing hair orientation defects (U. Weber and M. Mlodzik, unpublished results). In the pilot screen, we noted dosage-sensitive modifications of the phenotype with *Vang^{stbm-6}* and *Vang^{stbm-X}*, *fmi/stan^{frz3}*, *fmi/stan¹⁹²*, and *fmi/stan^{E59}*, while most other core *PCP* genes did not modify the phenotype significantly as heterozygotes. Alleles tested that did not modify were *fz*: R52 or 23, P21 or 21, R54 or 25, and F31 or 13; *dsh*: V26 or 3, A3, 477, and A21; *dgo*: 380, 308, and 269; *nemo* (*nmo*; *Nlk* in vertebrates): E33, DB, and P1; *fat*: *l(2)fd* or 8, *G-rv*, and *k07918*; *par-6^{Δ226}*; *aPKC*: *k06403*; *scribbled* (*scrib*): 673 and 1; *lethal(2)giant larvae* (*l(2)gl*): *4w3* and 4; *Epidermal growth factor receptor* (*Egfr*): *top-18A* and *CO* or *f24*; *kayak* (*kay*)/*Dfos*: 1 and *Df(3R)ED6315*; *pnt*: Δ88, 2, and 19099; *Jra/Djun*: *RC46* and 2 or *IA109*; and *Notch* (*N*): *55e11* and *Df(1)N-5419*. All crosses were grown at 25° unless otherwise noted. *bazooka* (*baz*)/*D-Par3*, *Delta* (*DI*), *ds*, and *anterior open* (*aop*)/*yan* showed significant modification of the eye phenotype, but only with some alleles (see also below). The photoreceptor arrangement/rhabdomere pattern was visualized by the *Rh1-GFP* transgene (Pichaud and Desplan 2001) (see Figure 1, A–E for examples).

In the wing, *stbm/Vang* and *fmi/stan* showed modification of *pk^{-/+}*, *sev-GAL4*, *UAS-dgo/+* wing *PCP* defects with two alleles each. No robust modification was found with *fz*, *dgo*, *dsh*, *fat*, *ds*, *scrib*, *par-6*, *l(2)gl*, *aPKC*, *nmo/Nlk*, *baz/D-Par3* and *Notch* (for alleles see above).

In the deficiency screen, 32% of the *DrosDel* deficiencies (Ryder *et al.* 2007) showed an external modification. A total of 5.6% of these were excluded due to non-*PCP* effects in the *Rh1-GFP* assay. Regions of the genome that showed robust modification in two independent experiments were further screened with smaller, subdividing, and/or partially

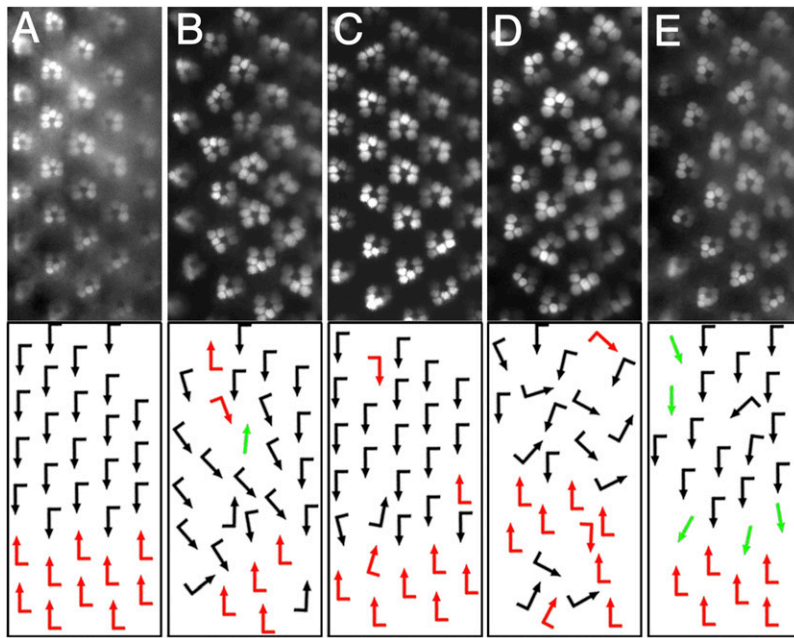
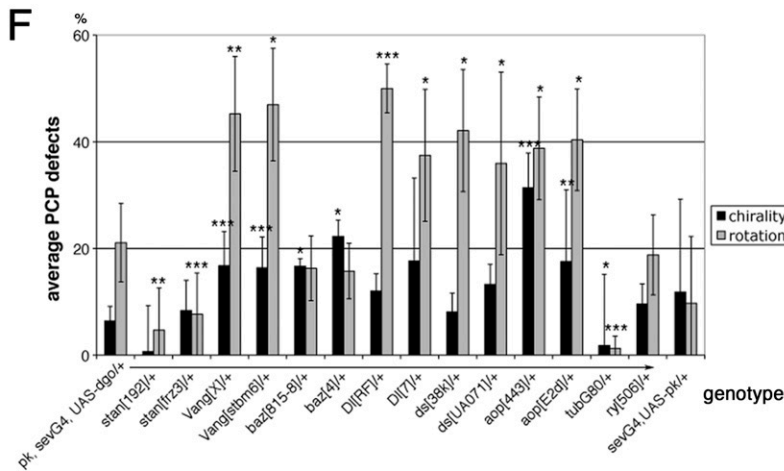


Figure 1 Ommatidial PCP orientation defects induced by Dgo or Pk overexpression and dominant modifications in the pilot screen. (A–E) *Rhodopsin1-GFP* (*Rh1-GFP*) pictures of rhabdomere patterns are shown on top and schematic arrows representing ommatidial orientation at bottom; dorsal is up and anterior to the left in these and all subsequent figures. The following genotypes are shown: wild type (A), *pk/+*, *UAS-dgo/+*, *Rh1-GFP/+*; *sev-GAL4/+* (referred to as *sev-GAL4*, *UAS-dgo*) (B), *stan^{frz3}/+*, *pk/+*, *UAS-dgo/+*, *Rh1-GFP/+*; *sev-GAL4/+* (C), *Vang^{stbm-X}/+*, *pk/+*, *UAS-dgo/+*, *Rh1-GFP/+*; *sev-GAL4/+* (D), and *UAS-Pk/+*, *sev-GAL4/+*, *Rh1-GFP/+* (referred to as *sev-GAL4*, *UAS-pk*) (E). Quantifications of interactions are shown in F. Black and red arrows indicate the two chiral ommatidial forms, and green arrows represent nonchiral, symmetrical ommatidia. Note that *stan^{frz3}/+* suppressed *sev-GAL4*, *UAS-dgo* rotation defects (C and F) and *Vang^{stbm-X}/+* enhanced *sev-GAL4*, *UAS-dgo* (D and F) chirality and rotation defects. Quantifications of additional candidate genes tested in pilot screen, showing significant modification: *bazooka* (*baz*)/*D-Par3*, *Delta* (*DI*), *dachsous* (*ds*), and *aop/yan* (F) (**P* < 0.06, ***P* < 0.01, and ****P* < 0.005; three to four eyes and 63–173 ommatidia were scored for each genotype). Chirality and rotation defects were counted independently; negative controls did not modify *sev-GAL4*, *UAS-dgo* and *GAL80^{ts}* abolished the phenotype (F).



overlapping deficiencies (including the Exelixis collection, Parks *et al.* 2004, or cytologically mapped deficiencies). Complementation crosses between deficiencies and mutant alleles were performed as controls. For some DrosDel deficiencies the interacting genes were identified by exclusion, as not all genomic regions within the original deficiency were uncovered by the Exelixis collection or other deficiencies. *UAS-RNAi* stocks from VDRC (Dietzl *et al.* 2007) and NIG were subsequently used to test individual genes within the respective genomic regions via loss-of-function (LOF) studies. The candidate genes were knocked down by *UAS-RNAi* transgenes using *decapentaplegic* (*dpp*)-*GAL4*, *engrailed* (*en*)-*GAL4*, and *apterous* (*ap*)-*GAL4* drivers for the wing and *sev-GAL4* for the eye. If tissue-specific RNAi knockdown produced PCP defects, we increased the phenotype by coexpressing *UAS-dicer2* and/or, increasing transgene copy numbers or by elevating the temperature to enhance the activity of the *GAL4/UAS* system.

Specific fly strains used:

sev-GAL4 (Basler *et al.* 1989), gift from K. Basler; *Rh1-GFP*, gift from F. Pichaud (Pichaud and Desplan 2001); *UAS-dgo*; *sev-GAL4* (K. Gaengel and M. Mlodzik, unpublished results); *UAS-pk^{sple}*, gift from D. Gubb, (Gubb *et al.* 1999); *Vang^{stbmX}* gift from Nuria Paricio; DrosDel deficiencies were received from Szeged (now distributed by the Bloomington Stock Center, Ryder *et al.* 2007); Exelixis deficiencies (distributed by FlyBase, were from Harvard University/Exelixis) (Parks *et al.* 2004); *sev-Dsh* (*2x*) and *sev-Fz* (Boutros *et al.* 1998).

UAS-RNAi lines were obtained from VDRC (Dietzl *et al.* 2007) and the NIG Fly Stock Centers. All other stocks were received from the Bloomington Stock Center.

Imaging and histology

Adult flies were initially inspected and evaluated on a Zeiss stereo microscope at $\times 66$ magnification for external eye and wing phenotype modification. The internal rhabdomere pattern was documented on a Zeiss Axioscope2 plus with a $\times 40$ water immersion lens at $\times 400$ magnification with UV light illumination. Concentric pictures of four individual eyes were evaluated and a total of 80–160 ommatidia were scored independently for rotation and chirality defects and statistically analyzed by *t* test. Wings were mounted in 80% glycerol in 1 \times PBS (Wu *et al.* 2004) and wing hair orientation defects analyzed for both surfaces of 4–10 wings. Tangential eye sections were prepared as described (Tomlinson and Ready 1987).

Results

Establishment of genotypes and pilot screen

Several genetic modifier screens addressing PCP have been performed in the past with a focus on the *trans*-membrane proteins *fz* and *stbm/Vang* (for example Rawls and Wolff 2003; Strutt and Strutt 2003), while the cytoplasmic components have been less explored. In particular, *dgo* and *pk* have not yet been used as screening tools, but are of specific interest due to their antagonistic relationship and opposing effects on Fz–Dsh/PCP signaling (Jenny *et al.* 2005).

To identify new regulatory factors related to PCP establishment that could either act on Dgo or Pk, affect Fz–Dsh/PCP signaling in general, or also function as effectors of the PCP pathway, we employed the *GAL4-UAS* system (Brand and Perrimon 1993) to overexpress Dgo and Pk. To screen both eye and wing tissues, we used a *sevenless* (*sev*-enhancer) heat-shock (*hs*)-promoter–*GAL4* (see *Materials and Methods*) (Basler *et al.* 1989) that drives expression in the eye transiently at high levels in the R3/R4 photoreceptor precursor pair at a time when PCP is being established (Strutt *et al.* 1997; Boutros *et al.* 1998) and at low levels in other tissues including the wing (due to the presence of basal level of expression from the *hs*-promoter, Figure 2, C and D). To test whether these genotypes were sensitive and specific enough for such an assay, we tested mutant alleles (see *Materials and Methods*) of the known Fz/PCP core components (reviewed in Adler 2002; Strutt 2003; Klein and Mlodzik 2005; Seifert and Mlodzik 2007), the parallel acting Fat/Ds PCP pathway (Matakatsu and Blair 2004; Casal *et al.* 2006; Lawrence *et al.* 2007; Simon *et al.* 2010), or the apicobasal (A/B)-polarity factors that are known to interact with PCP proteins (Djiane *et al.* 2005; Courbard *et al.* 2009). Furthermore, we tested the consistency of our imaging and scoring methods by examining the *rhodopsin1-GFP* rhabdomere marker (Pichaud and Desplan 2001) (*Materials and Methods*) for PCP-associated rhabdomere orientation defects (Figure 1, A–F) and hair orientation defects by microscopic inspection (Figure 2, C–F). In *sev-GAL4, UAS-dgo*, and *sev-*

GAL4, UAS-pk eyes (referred to as the screen genotypes), ommatidia showed chirality and rotation defects (Figure 1, B, E, and F and *Materials and Methods*). In *sev-GAL4, UAS-dgo* wings, cellular hairs were misoriented in the region between the anterior wing margin and longitudinal vein L3 (Figure 2D), while in *sev-GAL4, UAS-pk* wing hairs were partially misoriented between L2 and L3 on one surface (Figure 2C).

In the pilot screen, among the core PCP factors, removing a copy of *stbm/Vang* enhanced (Jenny *et al.* 2005) and, of *fmi/stan* suppressed, both eye and wing defects significantly (Figures 1, C, D, and F and 2, D–G). The fact that *stbm/Vang* modified the *dgo* GOF background is consistent with earlier data (Jenny *et al.* 2005). The observation that *fmi/stan* acted as a dominant suppressor in both tissues and the genetic effect of *fmi/stan* acting in opposition to *stbm/Vang* has not been observed but is consistent with current models (see *Discussion*). Of the other PCP-related genes tested, we observed that some but not all alleles of *ds* and *Delta* (*DL*), acting in R3/R4 specification (Cooper and Bray 1999; Fanto and Mlodzik 1999; Tomlinson and Struhl 1999) modified the *sev-GAL4, UAS-dgo* eye phenotype (Figure 1F; also below). Furthermore, the apicobasal determinant *bazooka* (*baz*)/*D-Par3* and the epidermal growth factor receptor (*Egfr*) effector *aop/yan* were found to enhance eye PCP defects significantly (Figure 1F). It has been shown independently that *baz/D-Par3* acts specifically on Fz: it positively regulates Fz levels/signaling in the eye and is upregulated during PCP signaling (Djiane *et al.* 2005) and that *dgo* overexpression in photoreceptor R4 promotes there the incorrect R3 fate (Jenny *et al.* 2005). In our experiment, reduction of *baz/D-Par3* function in *sev-GAL4, UAS-dgo*, presumably further abolished the difference between R3 and R4 cell fate and therefore enhances PCP chirality defects (Figure 1F). The *Aop/Yan* transcription factor is required in photoreceptor R3 to inhibit R4 fate (Weber *et al.* 2008). Here, reduction of *aop/yan* function in the context of *dgo* overexpression further reduced the cell fate difference between R3 and R4, causing more severe PCP defects (Figure 1F). Negative controls showed no effect in this assay (Figure 1F and data not shown), nor did other mutants tested (see *Materials and Methods*). As further control, *GAL80* abolished all effects, as it suppresses *GAL4*-mediated expression (Duffy 2002). No modifications were observed with *ds*, *DL*, *baz/D-Par3*, and *aop/yan* in the wing, which is consistent with eye-specific PCP functions of *DL*, *baz/D-Par3*, and *aop/yan* (Figure 1, legend and *Materials and Methods*).

Taken together, we have established effective tools to screen for novel PCP factors, which are both sensitive enough to identify suppressor- and enhancer-type interactions, but also stringent enough to only detect specific modifiers in the eye and the wing. We therefore utilized this set of tools to screen the genome of *Drosophila melanogaster* for new PCP regulators by lowering the copy number of gene intervals with deficiencies generated by *DrosDel* (Ryder *et al.* 2007).

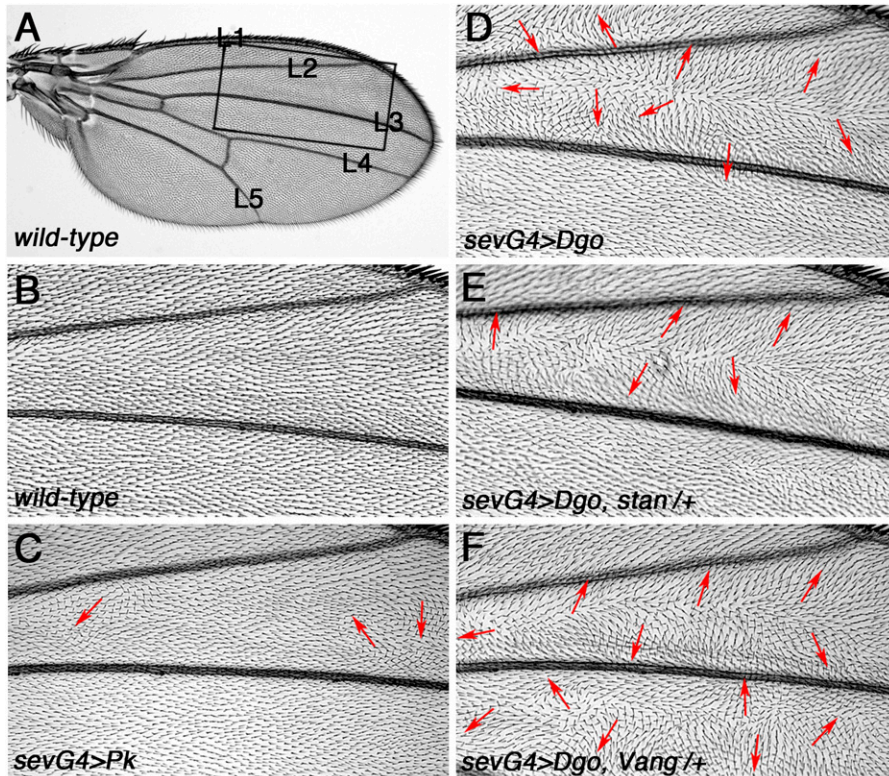


Figure 2 Wing hair orientation defects induced by Dgo or Pk overexpression and dominant modifications by *Vang/stbm* and *stan/fmi* in the pilot screen. (A and B) Wild-type wing overview (A) and detail (B, boxed area from A) as represented in all following panels. (C–F) Wing hair orientation defects between veins L1 and L4, highlighted by arrows in *sev-GAL4, UAS-dgo* (D), which are suppressed by *stan^{E59/+}* (E) and enhanced by *Vang^{stbm6/+}* (F). Wing hair defects in *sev-GAL4, UAS-pk* are milder (C). (G) Table summarizing dominant modification of wing hair orientations in *sev-GAL4, UAS-dgo* by candidate genes. Two alleles each of *stan/fmi* (E and G) and *Vang/stbm* showed the effect (F and G).

G

Genotype	Wing hair orientation in L1-L2 area	Wing hair orientation in L2-L3 area	Wing hair orientation in L3-L4 area	Interaction
<i>sev-GAL4, UAS-dgo+, +/+</i>	Multiple whirls on both surfaces	Multiple whirls on both surfaces	No effect	n. a.
<i>sev-GAL4, UAS-dgo+, stan^{E59/+}</i>	No effect	Multiple whirls on both surfaces	No effect	su
<i>sev-GAL4, UAS-dgo+, stan^{tr23/+}</i>	No effect	Multiple whirls on both surfaces	No effect	su
<i>sev-GAL4, UAS-dgo+, Vang^{6/+}</i>	No effect	Multiple whirls on both surfaces	Multiple whirls on both surfaces	enh
<i>sev-GAL4, UAS-dgo+, Vang^{X/+}</i>	No effect	Multiple whirls on both surfaces	Multiple whirls on both surfaces	enh

Deficiency screen

To identify new PCP regulatory factors, we screened both genotypes, *sev-GAL4, UAS-Dgo* and *sev-GAL4, UAS-Pk* (see *Materials and Methods* for details), testing these against the DrosDel deficiency collection for dominant modifications. In the primary screening, we examined the external appearance of adult compound eyes and wings for phenotypic suppression or enhancement (Table 1, Figure 3). For deficiencies displaying robust external modification(s) in either tissue, we examined in detail PCP orientation in the eye, using the internal *Rh1-GFP* rhabdomere pattern and wing hair orientation patterns in mounted wings (Table 1). A total of 195 deficiencies were screened in this manner, covering ~80% of the genome. Of these, 21% modified the internal PCP eye phenotype and 21% modified the wing phenotype. A total of 11% showed effects in both tissues and 8.5% affected both genotypes (Table 1). Those deficiencies affecting both genotypes were considered high-priority candidates and were analyzed further. A total of 68% of the

deficiencies did not show an effect (listed in [Supporting Information, Table S1](#)).

The initial genomic region responsible for an interaction was narrowed down by using smaller, subdividing deficiencies from the Exelixis collection (Parks *et al.* 2004) or partially overlapping cytologically mapped deficiencies (Figures 3 and 4). The same *Rh1-GFP* eye patterning analysis was used to confirm and refine the genomic region of interaction (see Figure 1). Many initially defined interactions were confirmed by such rescreening with smaller deficiencies (Table 2 and example shown in Figure 4A). In a small number of cases, however, we could not isolate the interaction in that manner, *e.g.*, the large deficiency was fully covered by subdividing deficiencies, but none of these reproduced the original interaction (Table 2, *Df(1) ED6957*, *Df(3L)ED207*, and *Df(3R)ED5623*). In such cases, it is likely that a combination of two or more genes caused the modification, which could not be mapped down to a single locus or the deficiencies harbored mutations outside their assigned coverage that were responsible for the initial effect.

Table 1 List of DrosDel deficiencies, which showed external modification of the *dgo* or *pk* induced PCP GOF phenotypes in the eye and/or wing and their analysis by *Rh1-GFP* and wing hair orientation assessment

DrosDel Df	sev-GAL4, UAS- <i>dgo</i> +			sev-GAL4, UAS- <i>pk</i> +		
	External eye	<i>Rh1-GFP</i> eye	Wing	External eye	<i>Rh1-GFP</i> eye	Wing
<i>Df(1)ED6720</i>	Enh 2x	Enh rota 2x	M enh 2x	ND	Enh rota, chir	M su
<i>Df(1)ED6727</i>	Enh	Enh rota 2x	No	ND	Enh rota	ND
<i>Df(1)ED6957</i>	Enh 2x	Enh rota 2x	Enh 2x	ND	No	Su
<i>Df(1)ED7161</i>	Enh 2x	Enh rota, chir 2x	Enh 2x	ND	ND	ND
<i>Df(1)ED447</i>	Enh 2x	Enh rota 2x	No 2x	ND	No	M su
<i>Df(1)ED7441</i>	No	Su chir	ND	Enh	Su chir	ND
<i>Df(1)ED7374</i>	Enh	Enh rota	ND	ND	ND	ND
<i>Df(1)ED7147</i>	Enh	Enh rota	ND	No	Su chir	ND
<i>Df(1)ED7344</i>	No	Enh rota	ND	Enh	No	ND
<i>Df(1)ED6521</i>	Enh	Enh rota	ND	Enh	No	ND
<i>Df(1)ED6443</i>	No	No	ND	Enh	No	ND
<i>Df(2L)ED62</i>	Enh 2x	Enh rota, chir 2x	M enh	ND	No	Su
<i>Df(2L)ED623</i>	Enh 2x	Enh rota, chir 2x	Enh 2x	ND	No	M su
<i>Df(2L)ED775</i>	Enh	Variable	No	ND	ND	ND
<i>Df(2L)ED784</i>	M enh	Variable	M enh	ND	Enh rota, chir	M su
<i>Df(2L)ED793</i>	M enh 2x	Enh rota	No 2x	ND	Enh rota, chir	M su
<i>Df(2L)ED1203</i>	Enh 2x	No	M enh	ND	Not scorable	No
<i>Df(2L)ED1315</i>	M enh	Enh rota 2x	Enh 2x	ND	Enh rota, chir	M su
<i>Df(2R)ED1552</i>	Enh	No	No	ND	ND	ND
<i>Df(2R)ED1618</i>	Enh 2x	Enh rota	S enh 2x	ND	Enh rota, chir	Enh
<i>Df(2R)ED1673</i>	S enh 2x	Enh rota, chir 2x	Enh 2x	ND	Enh rota, chir	M enh
<i>Df(2R)ED1715</i>	S enh 2x	ND	No	ND	ND	ND
<i>Df(2R)ED1742</i>	No 2x	No	Enh 2x	ND	No	Su
<i>Df(2R)ED2308</i>	M enh	Enh rota, chir	Enh	ND	No	M enh
<i>Df(2R)ED3791</i>	Enh 2x	Variable	Enh 2x	ND	No	No
<i>Df(2R)Exel6076</i>	Nd	Enh rota	ND	ND	Su chir	ND
<i>Df(2R)ED2247</i>	Nd	Enh rota	ND	ND	No	ND
<i>Df(2R)ED1725</i>	Nd	Enh rota	ND	ND	Su chir	ND
<i>Df(2R)ED1791</i>	Nd	Enh rota	ND	ND	Enh chir	ND
<i>Df(3L)ED201</i>	Enh 2x	Enh rota 2x	No 2x	ND	No	Su
<i>Df(3L)ED207</i>	Enh 3x	Enh rota 2x	Enh	ND	No	Su
<i>Df(3L)ED4284</i>	M enh 2x	Variable	Enh 2x	ND	No	M su
<i>Df(3L)ED4293</i>	Enh 2x	No	M enh	ND	ND	M su
<i>Df(3L)ED4483</i>	No 2x	No	Enh 2x	ND	No	No
<i>Df(3L)ED4502</i>	Enh	ND	Enh	ND	ND	ND
<i>Df(3L)ED4543</i>	M enh	Variable	Enh	ND	ND	ND
<i>Df(3L)ED220</i>	Enh 2x	Enh rota	M enh	ND	No	M su
<i>Df(3L)ED230</i>	M enh 2x	Enh rota 2x	Enh 2x	ND	Lethal	Lethal
<i>Df(3L)ED5017</i>	M enh 2x	Enh rota 2x	Enh 2x	ND	No	Su
<i>Df(3L)ED6279</i>	No	Enh rota	ND	Enh	Enh rota	ND
<i>Df(3L)ED4177</i>	No	No	ND	Enh	Enh rota, chir	No
<i>Df(3R)ED7665</i>	Enh 2x	Enh chir 2x	Enh 2x	ND	No	No
<i>Df(3R)ED5454</i>	Su	No	Su	ND	ND	ND
<i>Df(3R)ED5516</i>	Su 2x	No	No	ND	ND	ND
<i>Df(3R)ED5559</i>	M enh	Enh chir	Enh	ND	ND	ND
<i>Df(3R)ED5577</i>	Enh 2x	Enh rota, chir 2x	Enh 2x	ND	No	M su
<i>Df(3R)ED5623</i>	Enh 2x	Enh rota var	M enh 2x	ND	No	Enh
<i>Df(3R)ED5644</i>	Enh 2x	Enh rota, chir	M enh 2x	ND	Su chir	Su
<i>Df(3R)ED5705</i>	Enh 2x	Variable	Enh 2x	ND	Enh rota, chir	ND
<i>Df(3R)ED10639</i>	Enh 3x	Enh rota	M enh 3x	ND	Su chir + rota	Su
<i>Df(3R)ED5938</i>	No	Variable	Enh	ND	Enh rota	ND
<i>Df(3R)ED5942</i>	Enh 2x	Enh chir 2x	Enh 2x	ND	Enh rota, chir	M su
<i>Df(3R)ED10845</i>	Enh 2x	No	M enh	ND	No	Su
<i>Df(3R)ED6076</i>	Enh 2x	Enh rota, chir	No	ND	No	No
<i>Df(3R)ED6096</i>	Enh	No	S enh	ND	Enh rota, chir	ND
<i>Df(3R)ED6361</i>	M enh 2x	Variable	M enh	ND	No	No
<i>Df(3R)ED6085</i>	No	No	Enh	Enh	No	ND
<i>Df(3R)ED5296</i>	Enh	Enh rota, chir	Enh	ND	No	ND
<i>Df(3R)ED6052</i>	ND	Su rota, chir	Enh	ND	No	ND

(continued)

Table 1, continued

DrosDel Df	<i>sev-GAL4, UAS-dgo/+</i>			<i>sev-GAL4, UAS-pk/+</i>		
	External eye	<i>Rh1-GFP</i> eye	Wing	External eye	<i>Rh1-GFP</i> eye	Wing
<i>Df(3R)ED7665</i>	ND	Enh rota	ND	ND	ND	ND
<i>Df(3R)ED5612</i>	ND	Enh rota	ND	ND	ND	ND
<i>Df(3R)ED6220</i>	ND	Enh rota	ND	ND	Su chir	ND

Each DrosDel deficiency that showed an interaction was listed and strong interactors were analyzed further in detail for interaction with *sev-GAL4, UAS-dgo* and *sev-GAL4, UAS-pk* in the eye and wing. Some interactions were tested repeatedly, indicated by 2x. Interactions were categorized as Enh, enhanced; M, mildly; S, strongly; Su, suppressed; No, no interaction; ND, not determined. *Rh1-GFP* interactions were listed as enhanced or suppressed for rotation (rota) and/or chirality (chir) defects, and some effects were variable.

Additionally, we observed that some larger deficiencies were not fully covered by smaller ones, in which case we postulated that the remaining uncovered genes were responsible for the original interaction. This was indeed the case and was confirmed for *Df(1)ED447*, *Df(2L)ED1315*, and *Df(3R)ED7665* (Table 2 and example shown in Figure 4B; see also below). Among the deficiencies identified as modifiers, two uncovered genes with a previously known PCP function: *ds* and *Dl* (an eye-specific PCP factor) within *Df(2L)ED62* and *Df(3R)ED5942*, respectively. Their LOF alleles, *ds^{UA071}* and *Dl^{RF}*, confirmed the genetic interaction originally found with the large deficiencies (Table 2, Figure S1), which was consistent with data observed in the pilot screen (Figure 1F, see above). We did not recover other known PCP genes in the deficiency screen (see Discussion).

Since *pk* and *dgo* act at the level of *dsh*, we further tested whether any of the identified deficiencies (Table 1) interacted with *sev-dsh* (Boutros *et al.* 1998) in the eye. Unfortunately, the *Rh1-GFP* rhabdomere pattern did not resolve into sharp pictures in this genetic background and therefore only external modifications could be used as selection criteria. Two deficiencies, *Df(2L)ED793* and *ED(3R)5644*, displayed an interaction and were confirmed by eye sections to be suppressors of *sev-dsh* (Figure S2). In analogy, we also tested for modifications of *sev-fz*, *Rh1-GFP*, but none of the isolated deficiencies displayed a strong modification of this background.

For further analysis, we focused on the interacting genomic regions that showed an effect with both screen genotypes and/or in both tissues.

Identification and loss-of-function analyses of new PCP candidate regulators

The narrowing down of the initial genomic regions via subsequent screening with smaller deficiencies allowed us to define a small set of potential candidate genes for most interacting regions (Figure 3 and Table 2). These were then tested individually, each with *UAS-RNAi* transgenic flies in direct LOF function studies for PCP defects. Each candidate gene was first analyzed microscopically for eye PCP defects, with *UAS-RNAi, sev-GAL4, Rh1-GFP*. To increase the phenotypes observed, further crosses were set up in combination with *UAS-dcr2*, or the copy numbers of the *GAL4/UAS* constructs and/or the temperature were increased. Such flies were then analyzed in more detail in adult eye sections (Figure 5). For phenotypic analyses in the wing, specific *GAL4* drivers (see Materials and Methods) were used in combinations as described above for the eye (Table 3). The individual genes that showed PCP related LOF defects were then tested via *UAS-RNAi* in the original genetic backgrounds employed in the screen to confirm that the interaction within a given genomic region was caused by gene dosage reduction of the respective factor (Table 2). In this manner, within the 13 DrosDel deficiencies identified originally, we confirmed and isolated the interaction to 11 individual genes (Table 2).

Phenotypes observed in the eye included classical PCP defects represented by either rotation (Figure 5F) or chirality (Figure 5H) defects, or both (Figure 5, A, B, and D); they often occurred in combination with loss of photoreceptors, which is also observed in *dsh* LOF eyes, for example (Boutros *et al.* 1998). In the wing, phenotypic analyses again revealed classical PCP defects, like misoriented cellular hairs (Figure 6, D and I)

Screen DrosDel deficiencies for *sev-Gal4, UAS-dgo* and *sev-Gal4, UAS-pk* modifiers in the eye and wing

↓

Rescreen with smaller deficiencies which subdivide original deficiency and determine candidate genes in the interacting intervals

↓

Test candidate genes by RNAi for loss of function PCP defects in the eye and wing

↓

Confirm that identified gene is reproducing initial genetic interaction with *prickle* and *diego*

Figure 3 Overview of the PCP screen. Flow chart of the screening procedure, starting from the large DrosDel deficiencies.

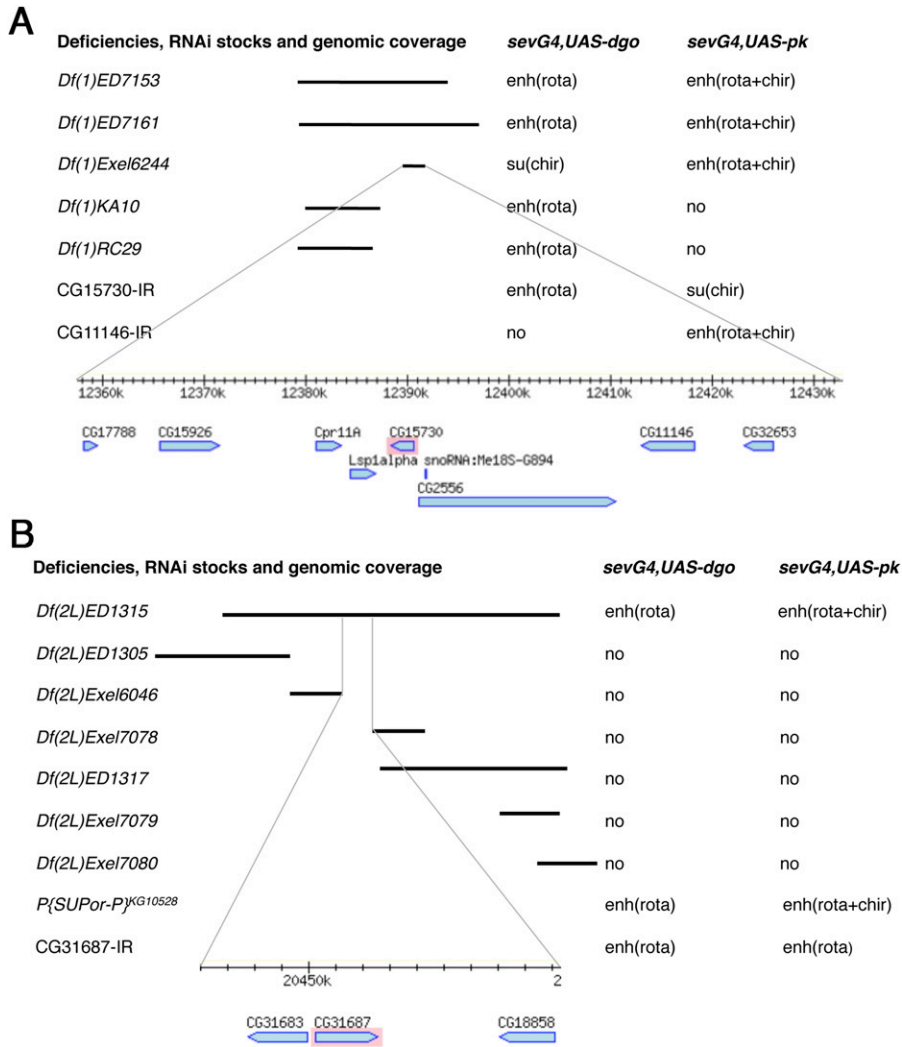


Figure 4 Single gene identification strategies for two DrosDel deficiencies, *Df(1)ED7161* and *Df(2L)ED1315*. Deficiencies and their coverage indicated by black bars are shown on the left and their genetic interactions are listed on the right. Fine lines at the bottom of each panel connect to a genomic map for the area that was tested by RNAi's (based on "MapBrowse, FlyBase"). (A) Mapping several interaction areas in *Df(1)ED7161*, which enhanced ommatidial rotation defects of *sev-GAL4, UAS-dgo* and enhanced rotation and chirality defects of *sev-GAL4, UAS-pk*. Two different genomic areas accounted for these effects, as identified by *Df(1)KA10* and *Df(1)RC29* for one of the interaction and *Df(1)Exel6244* for the other. *Df(1)Exel6244* was further studied since it modified both screen genotypes. *CG15730* and *CG11446* (now fused with *CG32653* and called *CG42251*) were found to reproduce, each a subset of the original genetic interaction. (B) For *Df(2L)ED1315*, mapping to a single gene was done by exclusion. DrosDel deficiency *Df(2L)ED1315* enhanced ommatidial rotation defects in *sev-GAL4, UAS-dgo* and enhanced both rotation and chirality defects in *sev-GAL4, UAS-pk*. Several overlapping or subdividing deficiencies were assayed for genetic interaction, but showed no modification of either genotype. This left three genes near the center of *Df(2L)ED1315* that were not covered by any of the smaller deficiencies. We therefore tested these three genes and found that RNAi for *CG31687* (an APC8 paralog) interacted similarly to *Df(2L)ED1315* with the two screening genotypes, as did a *P*-element insertion *KG10528* for *CG2508 (APC8/cdc23)*.

and/or clustered wing hairs (Figure 6, E–H). In addition, we observed wing margin defects/notches (Figure 6, A and B) and vein defects (Figure 6C). Both of the latter phenotypes might be associated with *Notch*-signaling (see *Discussion*). Most genes identified in this screen affected PCP in both tissues, the eye and wing, and few affected only one of the tissues (Table 3).

The molecular nature and features of these new PCP regulatory genes ranged from kinases, phosphatases, enzymes required for lipid biosynthesis or modification, to proteins involved in substrate degradation or modification. Among the kinases, *CG7004 (four wheel drive/fwd)* encodes a PI4kinase β , which has been shown to be required for male germ-line development (Polevoy *et al.* 2009), and *CG6963 (gilgamesh/gish)*, a casein kinase γ , known to be involved in many processes including Wnt signaling (Davidson *et al.* 2005), glial cell migration (Hummel *et al.* 2002), and spermatogenesis (Nerusheva *et al.* 2009). Phosphatases of the PAP2 family, *CG11426* and *CG11438*, were also identified. These belong to the same subfamily as *wunen* and *wunen2*, which control female germ-line development (Starz-Gaiano *et al.* 2001). *Fwd* and the PAP2 phosphatases are likely to act as lipid modification enzymes.

Interestingly, *CG31687*, an APC8 paralog, and *CG15283* encode proteins potentially involved in protein modification and/or degradation, possibly affecting substrate trafficking or localization, two features of likely importance in PCP establishment (Narimatsu *et al.* 2009). Scaffolding proteins encoded by *CG11146*, with SH3/SH2 domains, *CG1019* (Muscle LIM protein, Mlp), a LIM domain-containing protein (Clark *et al.* 2007) and *CG13388* (a kinase anchoring protein, Akap200) (Jackson and Berg 2002) were also isolated. Finally, proteins of unknown molecular nature encoded by *CG15730*, which is the fly ortholog of Mks1 (Meckel-Gruber syndrome 1), a gene mutated in human ciliary disease, and *CG10068*, which has been associated with cytokinesis in a cell-based genome-wide screen (Echard *et al.* 2004) round out the molecular features of the new PCP regulators (see *Discussion* for more details).

Genetic interactions with core PCP factors and Notch

The screen identified new PCP regulators as modifiers of a *dgo* or *pk* GOF phenotype. We also isolated factors that potentially modulate Notch signaling, as a few candidates showed notches or wing vein defects when knocked down

Table 2 Smaller deficiencies and individual genes, which confirmed original interactions

DrosDel deficiency	Subdividing deficiencies	Genes identified	<i>sev-GAL4, UAS-dgo</i> interaction	<i>sev-GAL4, UAS-pk</i> interaction
<i>Df(1)ED6957</i>	None ^a	ND		
<i>Df(1)ED7161</i>	<i>Df(1)ED7153</i>	CG17788 (no RNAi), CG15926 (no RNAi), CG2556, CG15730 , CG11146 , CG32653	CG15730: enh(rota)	Su (chir) ^b
	<i>Df(1)Exel6244</i>		CG11146: no ^b	Enh (rota + chir)
<i>Df(1)ED447</i>	None ^c	CG6461, CG6470, CG6335, CG10548, CG6481, CG15042, CG15047		
<i>Df(2L)ED62</i>	<i>Df(2L)Exel8003</i> <i>Df(2L)ED94</i> <i>Df(2L)ED49</i> <i>ds^{UA071}</i>	ds , CG2863		
<i>Df(2L)ED623</i>	<i>Df(2L)ED611</i> <i>Df(2L)ED647</i> <i>Df(2L)Exel8021</i>	CG13388 , CG13399, CG13400	Su (chir) ^b Enh (rota)	Su (rota + chir) ^b
<i>Df(2L)ED793</i>	<i>Df(2L)b87a25</i> <i>Df(2L)Exel6036</i> <i>Df(2L)Exel6035</i> <i>Df(2L)Exel8033</i>	CG15283 , CG4491, <i>noc</i> , CG15284, CG3474	Enh (rota)	No ^b
<i>Df(2L)ED1315</i>	None ^c	CG31683, CG31687 , CG18858	Enh (rota)	Enh (rota + chir)
<i>Df(2R)ED1618</i>	<i>Df(2R)ED1673</i>	Pk		
<i>Df(2R)ED1673</i>	<i>Df(2R)ED1618</i>	Pk		
<i>Df(3L)ED201</i>	<i>Df(3L)Exel6084</i> <i>fwd^{Df(3L)Exel9057}</i> <i>fwd^{hco1}</i>	CG7004	Enh (rota)	Enh (rota + chir) ^b
<i>Df(3L)ED207</i>	None ^a	ND		
<i>Df(3L)ED220</i>	<i>Df(3L)st[b11]^d</i>	ND		
<i>Df(3L)ED230</i>	<i>Df(3L)AI29</i> <i>Df(3L)AK1</i>	CG11438 , CG11426	ND	ND
<i>Df(3L)ED5017</i>	None ^e	ND		
<i>Df(3R)ED7665</i>	None ^c	CG14612 (no RNAi), CG1070 (no RNAi), CG1019 , CG10098 (ND), CG10068	Enh (rota) ^f	No
<i>Df(3R)ED5577</i>	<i>Df(3R)Exel7316</i>	ND		
<i>Df(3R)ED5623</i>	None ^a	ND		
<i>Df(3R)ED5644</i>	<i>Df(3R)Exel6267</i>	ND		
<i>Df(3R)ED5942</i>	<i>Df(3R)Cha9</i> <i>Df(3R)DI[RF]</i> <i>Df(3R)DI[7]</i>	DI		
<i>Df(3R)ED10639</i>	<i>Df(3R)Exel7329</i>	CG6889, CG6815, CG6814, CG6864, CG12785, CG6963 , CG31283	Enh (rota)	ND

The DrosDel and smaller deficiencies are listed in the first and second columns, respectively. The third column lists all genes that were tested by RNAi knockdown for PCP phenotypes. Genes that affected PCP when knocked down (compare Table 3) and reproduced the effects of the original deficiency are indicated in boldface type. *Df(2L)ED62* and *Df(3R)ED5642* covered *ds* and *DI*, respectively (compare Figure S1). Columns 4 and 5 list genes and the quality of their genetic interactions that reproduced the original genetic interactions with screen genotypes.

^a Full coverage by other dfs.

^b Genetic interaction is different from what was observed with initial deficiency.

^c Genes tested based on exclusion from smaller Dfs.

^d Approximately 60 gene overlap.

^e No smaller Dfs, close to centromere.

^f Genetic interaction is a subset of what was observed originally.

with *UAS-RNAi* (Figure 6, A–C; Table 3). As Notch signaling interacts with Fz/PCP core factors in the eye via *DI* upregulation (and *DI* was indeed one of the genes identified in the screen) this was consistent. We thus tested these candidate genes in a *Notch*^{-/+} background. However, we did not observe an enhancement of the *UAS-RNAi* induced eye or wing margin/vein phenotype in a *Notch* heterozygous background.

To get further insight into the potential role(s) of the newly identified PCP regulatory factors and/or to corroborate that some of them might act at the level of *dgo*, *pk*, and *dsh* within the PCP hierarchy, we next tested whether their func-

tion was sensitive to endogenous levels of *dgo*, *pk*, or *dsh*. To this end *UAS-RNAi*; *GAL4* stocks of the respective genes (with an eye- or wing-specific *GAL4* driver, see above) were analyzed for genetic requirements by crossing these to *dgo*, *pk*, *dsh*, *fat*, and *ds* mutants. Two genes were sensitive to halving the genomic dose of *dgo* and showed an enhancement of PCP defects in a heterozygous *dgo* background: *CG15730* and *CG15283* in the wing (Figure 7). The others did not display an equivalent interaction with either *dgo* or the other genes tested. Intercrossing *UAS-RNAi* transgenes of the new candidate PCP regulators/modifiers that caused similar wing

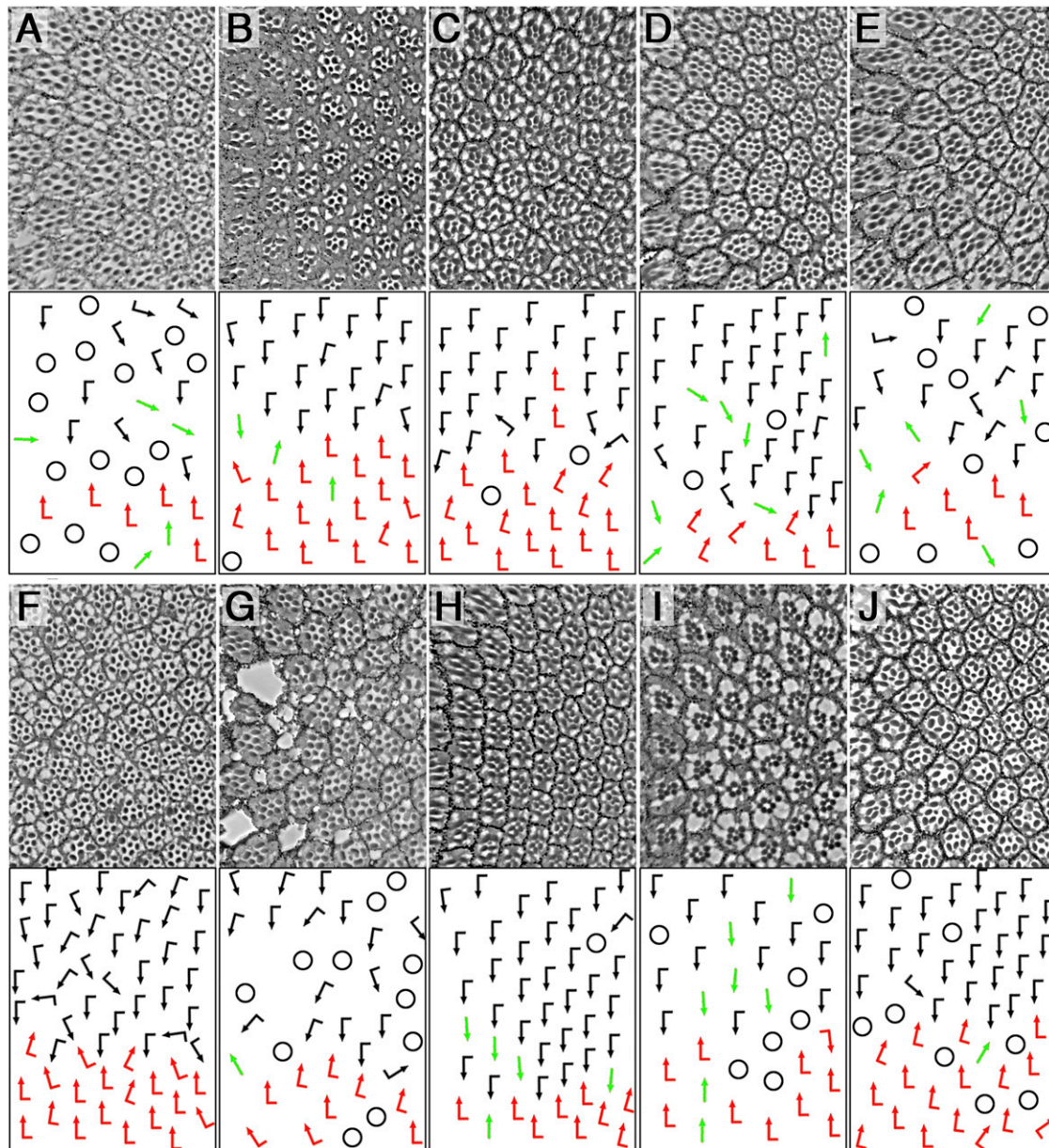


Figure 5 Eye PCP phenotypes of the novel candidate genes isolated in the screen. Top panels show tangential eye sections and bottom panels show a schematic of ommatidial orientation (arrows) (compare Figure 1A for wild type). Ommatidia with loss of photoreceptors or unscorable ommatidia are indicated by black circles in schematic. The following genotypes are shown: (A) *CG1019^{IR}; sev-GAL4 29°*, (B) *UAS-dcr-2/+; CG10068^{IR}/+; sev-GAL4/+ 25°*, (C) *CG15730^{IR}; sev-GAL4*, escaper at 19°, (D) *CG11146^{IR}; sev-GAL4 29°*, (E) *CG15283^{IR}/Y; sev-GAL4/+ 29°*, (F) *UAS-dcr-2/Y; CG31687^{IR}/+; sev-GAL4/+ 29°*, (G) *CG7004^{IR}; sev-GAL4/+* escapers 18°, (H) *UAS-dcr-2/Y; CG11438^{IR}/+; sev-GAL4/+ 29°*, (I) *UAS-dcr-2/+; CG13388^{IR}/+; sev-GAL4/+ 25°*, and (J) *UAS-dcr-2/Y; CG6963^{IR}/+; sev-GAL4/+ 29°*.

defects or fell into similar molecular function classes did not reveal specific enhancements, suggesting that they are not clustered functionally within a molecular complex.

The enhancement of *CG15283* by *dgo* heterozygosity was particularly robust (Figure 7, B and F) and thus we tested whether *dsh*, the genetic and molecular binding partner of *dgo*, also displayed interactions with *CG15283*. To this end we used *dsh* GOF and LOF eye phenotypes (as these are dosage sensitive and quantifiable) and asked whether levels of *CG15283* affect these. Strikingly, the *sev-Dsh* GOF pheno-

type is markedly suppressed by lowering the *CG15283* function via RNAi (Figure 8, A, B, and E) and comparable to the effect seen with *Df(2L)ED793*, which led us to identify *CG15283* (Figure S2). Accordingly, the PCP-specific hypomorphic *dsh¹* loss-of-function allele phenotype is strongly enhanced by *sevGAL4*, *CG15283^{IR}* gene knock down (Figure 8, C, D, and F). Thus, in both genetic scenarios, *CG15283* promotes Dsh function, being positively required for Dsh (this conclusion is also consistent with its genetic interactions in the original screen genotypes; see above).

Table 3 Summary of PCP defects in the eye and wing of candidate genes studied

DrosDel deficiency	Gene/RNAi transf. ID	Vertebrate homolog, molecular signature	<i>sev-GAL4</i>	<i>dpp-GAL4</i>	<i>en-GAL4</i>	<i>ap-GAL4</i>
<i>Df(1)ED7161</i>	<i>CG15730/19583</i>	Mks1, Basal body component	Rota, chir, notches, hair ori ^a	NE	NE	Mch
<i>Df(1)ED7161</i>	<i>CG42251/29634</i>	SH3/SH2 adaptor activity	Rota, chir ^b	NE	Vein defects ^c	NE
<i>Df(2L)ED62</i>	<i>CG2863 (Nle)/33574</i>	Regulator of Notch pathway, WD40 repeats	NE	Lethal	Lethal	Mch
<i>Df(2L)ED793</i>	<i>CG15283/ 28550</i>	—	Rota, chir ^b	Hair ori ^c	Hair ori ^c	NE
<i>Df(2L)ED793</i>	<i>CG15284 (pburs)/27141/2</i>	insect spec. partner of bursicone, ligand for G prot. coupled rec.	Chir ^d	Mch	Mch	Mch ^c
<i>Df(2L)ED1315</i>	<i>CG31687/21393</i>	APC8 paralog, component of the APC/C	Rota, chir	Mch	Hair ori	Mch ^c
<i>Df(3L)ED201</i>	<i>CG7004 (fwd)/27785/6</i>	PI4 kinase β	Rota, chir ^d	Lethal	Lethal/notches ^e	Mch ^f
<i>Df(3L)ED230</i>	<i>CG11438 (PAP2)/11438</i>	PAP2 type phosphatase	Rota, chir ^c	ND	ND	Vein ^c
<i>Df(3L)ED230</i>	<i>CG11426 (PAP2)/11426</i>	PAP2 type phosphatase	NE	ND	ND	Mch ^c
<i>Df(3R)ED7665</i>	<i>CG1019 (Mlp84B)/18594</i>	CSRP1, LIM domains	Loss, rota, chir ^{b,d}	NE	NE	NE
<i>Df(3R)ED7665</i>	<i>CG10068/15948</i>	—	Chir ^d	NE	Mch	NE
<i>Df(3R)ED10639</i>	<i>CG6963 (gish)/26003</i>	Casein kinase1 gamma	Loss, rota ^f	Mch ^c	Mch ^f	ND
<i>Df(2L)ED623</i>	<i>CG13388 (Akap200)/5647</i>	AKAP200/MESR2, protein kinase A binding	Loss, chir	NE	Vein defects ^d	NE

The first two columns list the deficiency and gene/RNAi. Third column indicates potential vertebrate homologs and/or molecular function. Further columns indicate which GAL4 driver caused phenotypes. Rota, ommatidial rotation defects; chir, ommatidial chirality defects; hair ori, wing hair orientation defects; mch, multiple cellular hairs; NE, no effect; ND, not done.

^a Increased copy number 19° escapers.

^b Increased copy number 29°.

^c 29°.

^d With UAS-dcr2.

^e Escapers with a 25°–18° temperature shift.

^f UAS-dcr2 at 29°.

gish/CK1γ regulates ommatidial rotation

Phenotypic analyses of *CG6963*, the gene encoding CK1γ (*gulgamesh/gish* in *Drosophila*) revealed specific features in eye PCP establishment. Moderate gene knockdown of *CG6963/gish* appeared to primarily affect ommatidial rotation (Figure 9A). Stronger knockdown of *gish* caused additional defects in photoreceptor specification including rare symmetrical ommatidia and R-cell loss (Figure 5J). These data are consistent with a role for *gish/CK1γ* in canonical Wnt signaling, as established in vertebrates for CK1γ (Davidson *et al.* 2005), and a potential (partially) redundant role (with CK1α and CK1ε) in PCP signaling as suggested earlier (Davidson *et al.* 2005; Zeng *et al.* 2005; Klein *et al.* 2006; Strutt *et al.* 2006).

To get more insight into the potential role of *gish* in ommatidial rotation, we (1) wished to confirm and refine the rotation phenotype in third instar imaginal discs during the actual process by analyzing a *gish* LOF allele and (2) tested for genetic interactions with other genes involved in ommatidial rotation. First, analyses of LOF clones in eye imaginal discs revealed that many clusters are underrotated in *gish* mutant tissue (Figure 9, D–D’).

Second, we asked whether a *gish* knockdown can affect other genes involved in ommatidial rotation. Among the core PCP factors, RNAi-mediated *gish* knockdown enhanced *sev-Fmi* (Figure 9, B and C; quantification in Figure S3B) and *sevG4*, *UAS-Fz* (not shown); in both cases the enhancement was specific to the rotation defects observed. This is consistent with the interaction detected in the original screen ge-

notype (a GOF *dgo* background) and it suggested a specific role for *gish* in ommatidial rotation. Next we asked whether any of the “rotation-specific PCP genes,” including *nemo* (*nmo*, Nlk in mammals) (Choi and Benzer 1994; Fiehler and Wolff 2008; Mirkovic *et al.* 2011), Rho-kinase (*dRok* in *Drosophila*) (Winter *et al.* 2001), or *zipper* (*zip*, myosin II) (Fiehler and Wolff 2007), display a specific interaction with *gish* in this process. Of these, *nmo* displayed an antagonistic interaction with *gish*; whereas *gish^{IR}* knockdown enhanced the *sevGAL4*, *UAS-Nmo* phenotype (Figure 9, E–F), the respective *sevGAL4*, *UAS-gish^{IR}* knockdown phenotype was suppressed by dosage reduction of *nmo* (*nmo^{DB}/+*; Figure 9G, see also Figure S3B for quantification). These data suggest that *Gish/CK1γ* acts in opposition to *Nmo/Nlk* and that a fine balance between the activities of these two kinases is required for normal ommatidial rotation to occur.

Discussion

Here we described a genetic screen to identify novel modifiers and regulatory factors linked to Fz/PCP signaling. We have used two mild GOF backgrounds of the cytosolic core components *Dgo* and *Pk* as screening tools, because they act antagonistically within the core Fz/PCP cassette. The screen relied on dosage sensitive interactions, a frequently used feature of mild PCP overexpression/GOF phenotypes (Strutt *et al.* 1997; Boutros *et al.* 1998; Strutt and Strutt 2003), and we used a combination of deficiency collections and transgenic RNAi strains to identify new PCP regulators.

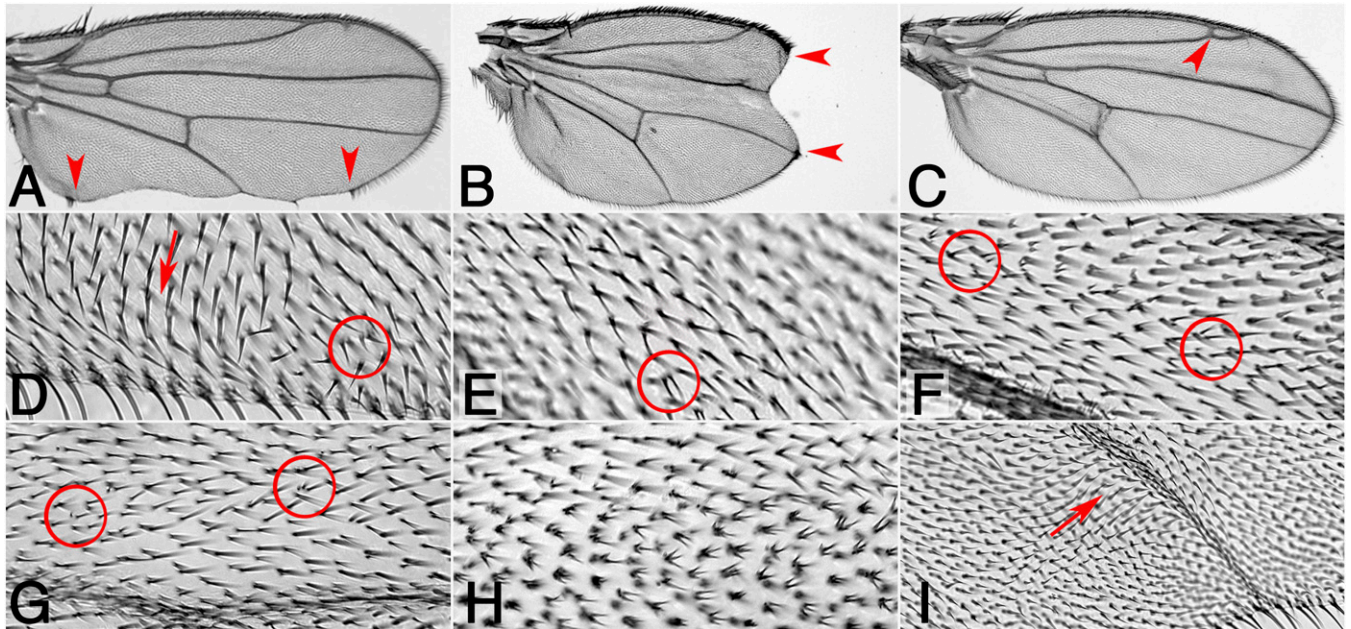


Figure 6 Wing PCP phenotypes of novel candidate genes. Wing phenotypes such as wing hair orientation defects, multiple cellular hairs, and notches were observed. For wild-type wing, compare Figure 2, A and B. Red arrowheads point to margin or vein defects. Wing hair orientation defects and multiple cellular hairs are indicated by arrows and circles, respectively. The following genotypes are shown: (A) *CG15730^{IR}; sev-GAL4* escapers 19°, (B) *en-GAL4/+; CG7004^{IR} /+ escapers* 18–25°, (C) *UAS-dcr-2/Y; ap-GAL4/+; CG1143^{IR} /+ escapers* 29°, (D) *CG15730^{IR}; sev-GAL4* 19°, (E) *UAS-dcr-2/+; ap-GAL4/+; CG7004^{IR} /+ 29°*, (F) *UAS-dcr-2/Y; en-GAL4/+; CG11146^{IR} /+ 29°*, (G) *CG31687^{IR} /+; dpp-GAL4/+ 29°*, (H) *en-GAL4/+; CG6963^{IR} /+ 29°C*, and (I) *CG15283^{IR} /Y; en-GAL4/+ 29°*. Wing defects with *sev-GAL4* driver are due to low level activity/overexpression in all tissues due to the *hs*-promoter in *sev-GAL4* (also *Materials and Methods*). Compare Table 3 for a summary of phenotypes for several *GAL4* drivers for each gene/RNAi of an original genetic interaction.

We first tested the genotypes of interest in a pilot screen with known PCP factors, other associated signaling pathway components (e.g., *Dl*), and negative controls. The positive candidates from the pilot screen indicated that the phenotypes were well within the appropriate sensitivity range for a dosage-dependent screen. In particular, the fact that *stbm/Vang* enhanced the *dgo* GOF phenotype supports previous studies and the existing model that Dgo promotes Fz–Dsh signaling activity, whereas *stbm/Vang* antagonizes it (Jenny *et al.* 2005). The fact that *stan/+* suppressed the *dgo* GOF phenotype is novel, but consistent with existing models, as Stan/Fmi is thought to contribute to anchoring Dgo at the membrane as part of the Fz–Dsh complex (Feiguin *et al.* 2001; Das *et al.* 2004; Strutt and Strutt 2007; Wu *et al.* 2008).

Our genome-wide screen has identified a set of genes with a broad range of functions, some of which were known to affect PCP (*ds* and *Dl*, see above for references) and a group of novel genes in the PCP context (see below). Generally, most of the genes identified were “hits” associated with *dgo*, and several of these not only modified the *dgo* GOF phenotype, but were also enhanced by *dgo* heterozygosity when knocked down via RNAi (Figure 7). We trust that all the genes identified via RNAi are specific (and not due to potential off-target effects), as they largely reproduced the genetic interaction(s) seen with the deficiencies (Table 2). As we narrowed down the genomic areas responsible for the genetic interactions, we sometimes observed

that the quality of a genetic effect changed. This could be due to separating several independent interacting genes that were initially causing an “additive effect” within the larger deficiencies or by separating genomic regulatory sequences that modify effects (Figure 4A, Table 2, and Figure S1).

Through the design of the screen we not only isolated dosage-sensitive interactors, but our approach directly led to the identification of genes that display PCP phenotypes in a loss-of-function (knockdown) scenario. As such, every new gene isolated is indeed required for PCP establishment and most of them act in eye and wing tissue, suggesting a general requirement. There might be tissue-specific hits in our screen (Table 1), which have not yet been characterized.

Besides *pk*, we were not able to identify other core Fz/PCP genes in the deficiency screen that showed a dose-dependent interaction in the pilot screen (*Vang/stbm* and *stan/fmi*). A possible explanation is that a single deficiency can harbor genes that act antagonistically and thus neutralize each other in a modification assay, e.g., *fmi/stan* resides near other genes that can affect PCP (e.g., *dgo* and *pipsqueak/psq*; Weber *et al.* 1995; Feiguin *et al.* 2001; Weber *et al.* 2008) and no interaction was seen with deficiency *Df(2R)ED2098*, which removes *fmi/stan*. Several of the newly identified genes fall into interesting functional categories that are either novel within the PCP regulatory machinery or may provide insight into new regulatory mechanisms. These include for example lipid modifications, factors associated with

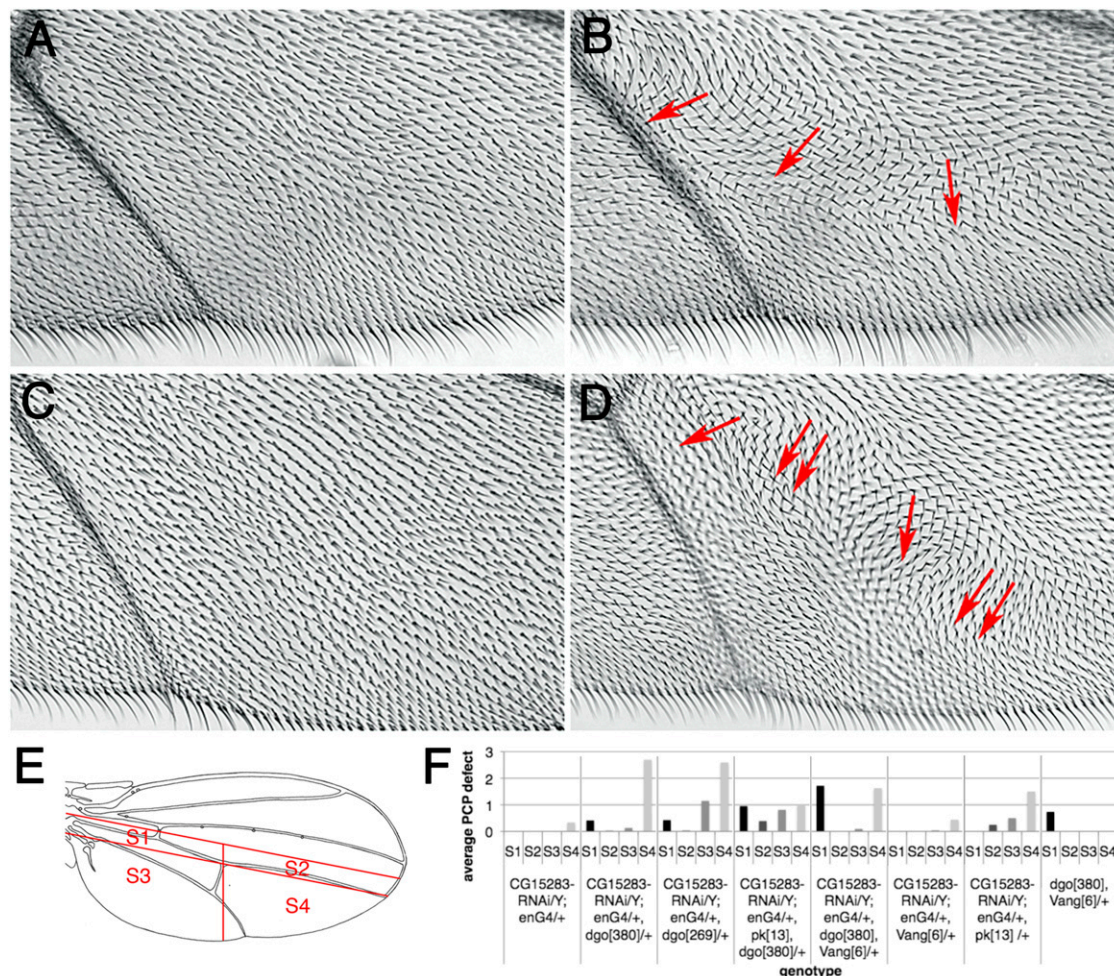


Figure 7 *CG15283* and *CG15730* dominantly interact with *dgo* loss of function. (A–D) Wing hair orientation in an area between longitudinal vein L4 and L5, controls (left, A and C) and dominant enhancement (*dgo*^{-/+}) (right, B and D) are shown. Red arrows highlight wing hair orientation defects. Double arrow indicates defects on both wing surfaces. (A) *CG15283*^{RNAi/Y}; *en-GAL4*^{+/+}; *pk*^{13/+} (*n* = 9) displayed wild-type orientation of hairs, whereas removal of one copy of *dgo* caused wing hair whirls in 89% of *CG15283*^{RNAi/Y}; *en-GAL4*^{+/+}; *dgo*^{380/+} (*n* = 9) (B). (C) *en-GAL4*^{+/+}; *pk*^{13/+}; *CG15730*^{RNAi/+} (*n* = 4) showed wild-type wing hair polarity, whereas reduction of *dgo* copy number enhanced the PCP defects (D) in 44% of *en-GAL4*^{+/+}; *dgo*^{380/+}; *CG15730*^{RNAi/+} wings (*n* = 9). (E–F) Quantification of the dominant interactions of *CG15283*^{RNAi}. Phenotypes were assessed in four sectors of the wing as indicated in drawing (E). Graph summarizing dominant interactions between *CG15283*, two *dgo* LOF alleles, and further modification by *pk* and *Vang/stbm* (*n* = 2–33 wings) at 30°. PCP defect of “1” corresponds to 10–20 misoriented wing hairs at a 45°–180° angle compared to surrounding wild-type hairs.

mammalian ciliopathies, and, presumably, protein stability/trafficking via ubiquitination (see below).

Functional features of new PCP regulators

The types of new genes recovered in the screen fall into several categories expanding the biochemical functions associated with PCP establishment in *Drosophila*. Three of the new genes, CG11426, CG11438, and *fwd*, encode lipid modification enzymes, with *fwd* encoding a PI4Kinaseβ (Polevoy *et al.* 2009) and the other two being PAP2-type phosphatases (Starz-Gaiano *et al.* 2001). These are intriguing new factors as lipid kinases and phosphatases could modulate the composition of the lipid microenvironment of the core PCP complexes and thus regulate their trafficking and/or stability at the plasma membrane among others (Weber *et al.* 2003; Simons *et al.* 2009). An aspect of lipid modification affecting core Fz/PCP signaling has recently been shown

to be important for the stabilization of Dsh membrane association and thus stabilization of the Fz–Dsh complex (Simons *et al.* 2009). As the phosphorylation state of the lipid heads often contributes to signaling by serving as protein binding sites, the identification of two lipid phosphatases and a lipid kinase suggests that some core PCP factors may prefer specific phosphorylation states of lipids, for either direct lipid binding or stabilization of the associated complexes.

A second functionally linked group consists of CG31687 and CG15283. CG31687 encodes a *Drosophila* APC8 paralog (*cdc23*), a component of the anaphase promoting complex/cyclosome (APC/C) (reviewed in Peters 2006). Strikingly, CG15283 genetically also interacted not only with core PCP factors but also with CG31687, thus forming a potential pair. While it has been suggested that ubiquitin-mediated modifications can regulate PCP in mice, with Smurf1/2 leading to Pk ubiquitination (Narimatsu *et al.* 2009), a ubiquitin link has

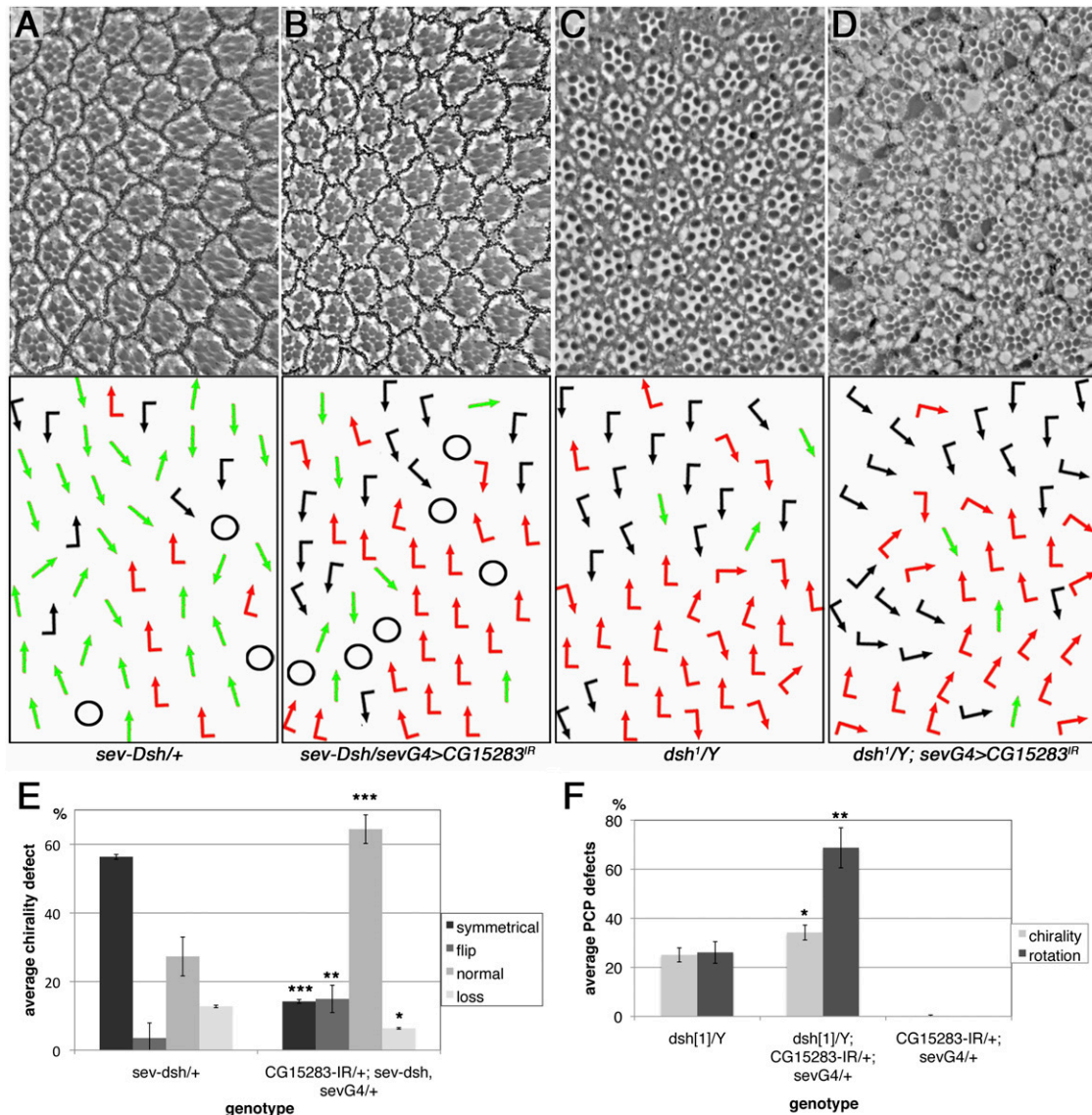


Figure 8 *CG15283* acts at the level of *dsh* promoting its activity. (A–D) Top panels show tangential eye sections and bottom panels, the respective schematic of ommatidial chirality/orientation (arrows) (compare Figure 1A for wild type and Figure 5). The following genotypes are shown: (A) *sev-dsh/+*, (B) *CG15283^{IR/+}; sev-GAL4/+; sev-dsh/+*, (C) *dsh^{1/Y}*, (D) *dsh^{1/Y}; CG15283^{IR/+}; sev-GAL4/+*. (E and F) Quantification of the above interactions, note suppression of *dsh* GOF PCP defects in *sev-dsh* (A, B, and E) and enhancement of the PCP-specific hypomorphic *dsh¹* LOF phenotype (C, D, and F) by *CG15283^{IR}* knockdown. (E) * $P < 0.007$, ** $P < 0.003$, and *** $P < 0.0001$, with $n = 568$ –893 ommatidia in four to five eyes. (F) * $P < 0.005$ and ** $P < 0.001$, with $n = 536$ –806 ommatidia in three to four eyes.

not yet been made in *Drosophila*. The potential involvement of the APC/C in noncell-cycle-associated cellular aspects like cell polarity (Peters 2002) is intriguing. In addition to its interaction with CG31687, CG15283 appears to be an interesting factor in its own right. Its phenotypic and genetic interactions with *dgo* and *dsh* (Figures 7 and 8) suggest that it functions in either modifying Dsh activity or affecting the balance between Dgo and Pk, which promote and antagonize Dsh function, respectively. Structure–function studies will be needed to reveal the molecular features of CG15283.

Three isolated genes fall into the category of scaffold proteins, CG1019 (*Mlp1*, a LIM domain-containing protein),

CG11146 (an SH2–SH3 domain-containing factor), and CG13388 (*Drosophila* Akap200). Scaffold proteins are common factors in protein complexes and thus the formation or stabilization of a PCP-specific complex or an associated complex is likely to require other such proteins. Akap200, although by name a PKA-associated factor in some contexts, also has non-PKA-mediated functions (Jackson and Berg 2002) and thus could well be involved in Fz/PCP signaling.

CG6963 is *Drosophila* CK1 γ , called *gilgamesh* (*gish*) in flies. Members of the casein kinase 1 family have been implicated in several aspects of canonical Wnt signaling (Davidson *et al.* 2005; Zeng *et al.* 2005; Klein *et al.* 2006;

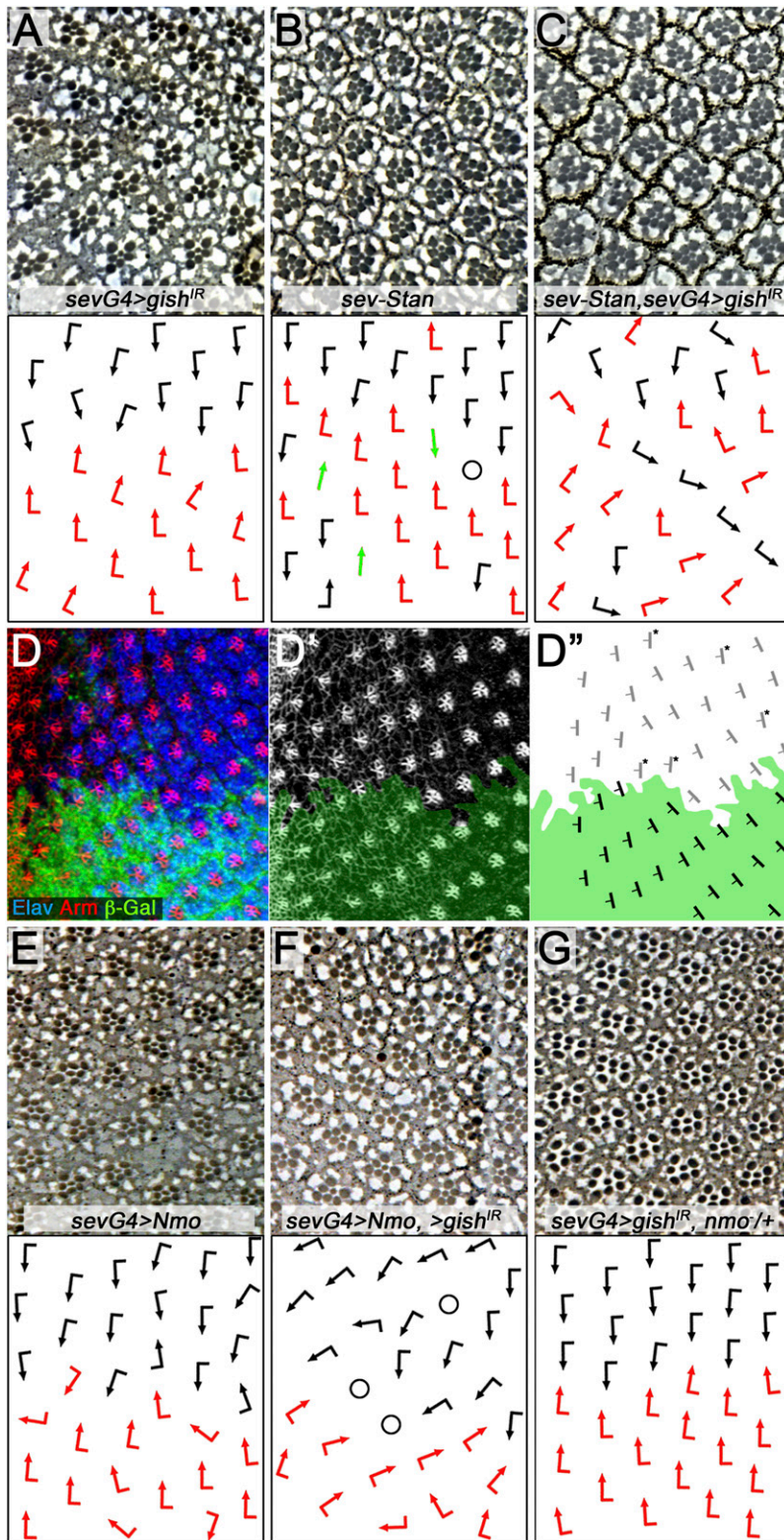


Figure 9 CG6963/CK1 γ affects rotation in the developing eye and interacts with *stan/fmi* and *nemo/Nlk*. (A–C and E–F) Tangential eye sections in top panels and the respective schematic representation of ommatidial orientation is shown at bottom (arrows are as in Figures 1 and 5). All crosses were performed at 25°. (D–D'') Eye imaginal disc containing a *gish*^{e01759} clone (marked by absence of GFP) stained for Elav (blue; marking all photoreceptor precursors) and Arm (red in D monochrome in D', highlighting cellular architecture by labeling the adherens junctions). D'' shows a schematic of rotation angles with the wild-type area indicated by green. Note several severely under-rotated clusters marked by asterisks. Eye sections of the following genotypes are shown: (A) *sev-GAL4/+*, CG6963^{IR/+}, (B) *sev-Fmi/+*, (B) *sev-Fmi/+*; *sev-GAL4/+*, CG6963^{IR/+}. Note enhanced rotation defects in C; for quantification see Figure S3B. (E) *sev-GAL4/+*, *UAS-Nmo/+*, (F) *sev-GAL4/+*, *UAS-Nmo/+*, CG6963^{IR/+} (note enhanced rotation defects as compared to E; for quantification see Figure S3B), (G) *sev-GAL4/+*, CG6963^{IR/+} *nmo*^{DB/+}, which is suppressed (compare to A).

Strutt *et al.* 2006) as well as in Fz/PCP regulation, in particular CK1 ϵ (Klein *et al.* 2006; Strutt *et al.* 2006) and CK1 α (Strutt *et al.* 2006). CK1 family members have been shown to phosphorylate Dsh (Klein *et al.* 2006; Strutt *et al.* 2006), and *gish* might act (at least) partially in a redundant manner

in Dsh (core Fz/PCP) regulation and hence was identified in the screen. In addition, we observed two specific PCP-associated phenotypes with CG6963/*gish* knockdown, which were also confirmed with LOF clones of existing mutant alleles. First, we detect a function in ommatidial rotation

and ommatidial clusters appear to rotate less in *gish* mutant tissue. This defect is accompanied by genetic interactions with Fz and Stan/Fmi among the core PCP genes. Furthermore, *gish* interacts with *nemo* (Mirkovic *et al.* 2011) in this context in a specific manner: Gish/CK1 γ and Nemo act in opposition to each other (Figure 9), suggesting that a fine balance between the activities of these two kinases is required for normal ommatidial rotation to occur. Second, *gish/CG6963* knockdown displays a high frequency of multiple cellular hairs, which is independent of a direct interaction with the core PCP factors (Gault *et al.* 2012).

The identification of CG15730 with a connection to PCP signaling is intriguing, as it encodes the *Drosophila* homolog of the Mks1 gene, a member of the Meckel-Gruber syndrome factors that are generally linked to ciliopathies in humans (Simons and Mlodzik 2008). PCP establishment in vertebrates has been linked to cilia positioning and function in several contexts (*e.g.*, Wallingford 2006; Park *et al.* 2008; Borovina *et al.* 2010). As epithelial cells in *Drosophila* are not ciliated, our observation that *dMks1/CG15730* interacts with core Fz/PCP factors and displays PCP defects by itself when knocked down suggests that cilia-associated factors are likely to be generally required for aspects of PCP establishment unrelated to ciliogenesis. As most of the genes linked to ciliopathies (*e.g.*, those associated with the Meckel-Gruber and Bardett-Biedl syndromes) are conserved in *Drosophila*, this observation suggests that analyses of other such genes in PCP establishment in *Drosophila* are warranted. CG10068, a novel protein of unknown function, has been linked to cytokinesis (Echard *et al.* 2004) and could thus also be interacting with cytoskeletal elements or associated proteins.

Acknowledgments

We thank K. Basler, C. Desplan, K. Gaengel, D. Gubb, N. Paricio, F. Pichaud, and the Nippon Institute of Genetics and Bloomington Stock Centers for fly strains, and Sophy Okello for technical help. We are grateful to Mei-Ling Chin and Lindsay Kelly for critical reading of the manuscript and all Mlodzik lab members for helpful comments throughout the course of this work. W. J. Gault was in part supported by T32 grants GM08553 and CA78207; P. Olguin was supported by a Pew Latin American Fellows postdoctoral fellowship. This work was supported by National Institutes of Health RO1 grant GM62917 to M. Mlodzik.

Literature Cited

- Adler, P. N., 2002 Planar signaling and morphogenesis in *Drosophila*. *Dev. Cell* 2: 525–535.
- Basler, K., P. Siegrist, and E. Hafen, 1989 The spatial and temporal expression pattern of *sevenless* is exclusively controlled by gene-internal elements. *EMBO J.* 8: 2381–2386.
- Bayly, R., and J. D. Axelrod, 2011 Pointing in the right direction: new developments in the field of planar cell polarity. *Nat. Rev. Genet.* 12: 385–391.
- Borovina, A., S. Superina, D. Voskas, and B. Ciruna, 2010 Vangl2 directs the posterior tilting and asymmetric localization of motile primary cilia. *Nat. Cell Biol.* 12: 407–412.
- Boutros, M., and M. Mlodzik, 1999 Dishevelled: at the crossroads of divergent intracellular signaling pathways. *Mech. Dev.* 83: 27–37.
- Boutros, M., N. Paricio, D. I. Strutt, and M. Mlodzik, 1998 Dishevelled activates JNK and discriminates between JNK pathways in planar polarity and *wingless* signaling. *Cell* 94: 109–118.
- Brand, A. H., and N. Perrimon, 1993 Targeted gene expression as a means of altering cell fates and generating dominant phenotypes. *Development* 118: 401–415.
- Casal, J., P. A. Lawrence, and G. Struhl, 2006 Two separate molecular systems, Dachshous/Fat and Starry night/Frizzled, act independently to confer planar cell polarity. *Development* 133: 4561–4572.
- Chen, W. S., D. Antic, M. Matis, C. Y. Logan, M. Povelones *et al.*, 2008 Asymmetric homotypic interactions of the atypical cadherin flamingo mediate intercellular polarity signaling. *Cell* 133: 1093–1105.
- Choi, K.-W., and S. Benzer, 1994 Rotation of photoreceptor clusters in the developing *Drosophila* eye requires the *nemo* gene. *Cell* 78: 125–136.
- Clark, K. A., J. M. Bland, and M. C. Beckerle, 2007 The *Drosophila* muscle LIM protein, Mlp84B, cooperates with D-titin to maintain muscle structural integrity. *J. Cell Sci.* 120: 2066–2077.
- Cooper, M. T. D., and S. J. Bray, 1999 Frizzled regulation of Notch signalling polarizes cell fate in the *Drosophila* eye. *Nature* 397: 526–529.
- Courbard, J. R., A. Djiane, J. Wu, and M. Mlodzik, 2009 The apical/basal-polarity determinant Scribble cooperates with the PCP core factor Stbm/Vang and functions as one of its effectors. *Dev. Biol.* 333: 67–77.
- Das, G., J. Reynolds-Kenneally, and M. Mlodzik, 2002 The Atypical Cadherin Flamingo Links Frizzled and Notch Signaling in Planar Polarity Establishment in the *Drosophila* Eye. *Dev. Cell* 2: 656–666.
- Das, G., A. Jenny, T. J. Klein, S. Eaton, and M. Mlodzik, 2004 Diego interacts with Prickle and Strabismus/Van Gogh to localize planar cell polarity complexes. *Development* 131: 4467–4476.
- Davidson, G., W. Wu, J. Shen, J. Bilic, U. Fenger *et al.*, 2005 Casein kinase 1 gamma couples Wnt receptor activation to cytoplasmic signal transduction. *Nature* 438: 867–872.
- Dietzl, G., D. Chen, F. Schnorrer, K. C. Su, Y. Barinova *et al.*, 2007 A genome-wide transgenic RNAi library for conditional gene inactivation in *Drosophila*. *Nature* 448: 151–156.
- Djiane, A., S. Yogev, and M. Mlodzik, 2005 The apical determinants aPKC and dPatj regulate Frizzled-dependent planar cell polarity in the *Drosophila* eye. *Cell* 121: 621–631.
- Donoughe, S., and S. DiNardo, 2011 dachshous and frizzled contribute separately to planar polarity in the *Drosophila* ventral epidermis. *Development* 138: 2751–2759.
- Duffy, J. B., 2002 GAL4 system in *Drosophila*: a fly geneticist's Swiss army knife. *Genesis* 34: 1–15.
- Echard, A., G. R. Hickson, E. Foley, and P. H. O'Farrell, 2004 Terminal cytokinesis events uncovered after an RNAi screen. *Curr. Biol.* 14: 1685–1693.
- Fanto, M., and M. Mlodzik, 1999 Asymmetric Notch activation specifies photoreceptors R3 and R4 and planar polarity in the *Drosophila* eye. *Nature* 397: 523–526.
- Feiguin, F., M. Hannus, M. Mlodzik, and S. Eaton, 2001 The Ankyrin repeat protein Diego mediates Frizzled-dependent planar polarization. *Dev. Cell* 1: 93–101.
- Fiehler, R. W., and T. Wolff, 2007 *Drosophila* Myosin II, Zipper, is essential for ommatidial rotation. *Dev. Biol.* 310: 348–362.

- Fiehler, R. W., and T. Wolff, 2008 Nemo is required in a subset of photoreceptors to regulate the speed of ommatidial rotation. *Dev. Biol.* 313: 533–544.
- Gault, W. J., P. Olguin, U. Weber, and M. Mlodzik, 2012 Drosophila CK1 γ , gilgamesh, Controls PCP-mediated Morphogenesis Through Regulation of Vesicle Trafficking. *J. Cell Biol.* 196: 605–621.
- Gubb, D., C. Green, D. Huen, D. Coulson, G. Johnson *et al.*, 1999 The balance between isoforms of the prickle LIM domain protein is critical for planar polarity in Drosophila imaginal discs. *Genes Dev.* 13: 2315–2327.
- Hummel, T., S. Attix, D. Gunning, and S. L. Zipursky, 2002 Temporal control of glial cell migration in the Drosophila eye requires gilgamesh, hedgehog, and eye specification genes. *Neuron* 33: 193–203.
- Jackson, S. M., and C. A. Berg, 2002 An A-kinase anchoring protein is required for protein kinase A regulatory subunit localization and morphology of actin structures during oogenesis in Drosophila. *Development* 129: 4423–4433.
- Jenny, A., J. Reynolds-Kenneally, G. Das, M. Burnett, and M. Mlodzik, 2005 Diego and Prickle regulate Frizzled planar cell polarity signalling by competing for Dishevelled binding. *Nat. Cell Biol.* 7: 691–697.
- Klein, T. J., and M. Mlodzik, 2005 Planar cell polarization: an emerging model points in the right direction. *Annu. Rev. Cell Dev. Biol.* 21: 155–176.
- Klein, T. J., A. Jenny, A. Djiane, and M. Mlodzik, 2006 CKIepsilon/discs overgrown promotes both Wnt-Fz/beta-catenin and Fz/PCP signaling in Drosophila. *Curr. Biol.* 16: 1337–1343.
- Lawrence, P. A., J. Casal, and G. Struhl, 2004 Cell interactions and planar polarity in the abdominal epidermis of Drosophila. *Development* 131: 4651–4664.
- Lawrence, P. A., G. Struhl, and J. Casal, 2007 Planar cell polarity: One or two pathways? *Nat. Rev. Genet.* 8: 555–563.
- Matakatsu, H., and S. S. Blair, 2004 Interactions between Fat and Dachsous and the regulation of planar cell polarity in the Drosophila wing. *Development* 131: 3785–3794.
- Mirkovic, I., W. J. Gault, M. Rahnama, A. Jenny, K. Gaengel *et al.*, 2011 Nemo kinase phosphorylates beta-catenin to promote ommatidial rotation and connects core PCP factors to E-cadherin-beta-catenin. *Nat. Struct. Mol. Biol.* 18: 132–142.
- Mlodzik, M., 1999 Planar polarity in the *Drosophila* eye: a multifaceted view of signaling specificity and cross-talk. *EMBO J.* 18: 6873–6879.
- Narimatsu, M., R. Bose, M. Pye, L. Zhang, B. Miller *et al.*, 2009 Regulation of planar cell polarity by Smurf ubiquitin ligases. *Cell* 137: 295–307.
- Nerusheva, O. O., N. V. Dorogova, N. V. Gubanova, O. S. Yudina, and L. V. Omelyanchuk, 2009 A GFP trap study uncovers the functions of Gilgamesh protein kinase in Drosophila melanogaster spermatogenesis. *Cell Biol. Int.* 33: 586–593.
- Park, T. J., B. J. Mitchell, P. B. Abitua, C. Kintner, and J. B. Wallingford, 2008 Dishevelled controls apical docking and planar polarization of basal bodies in ciliated epithelial cells. *Nat. Genet.* 40: 871–879.
- Parks, A. L., K. R. Cook, M. Belvin, N. A. Dompe, R. Fawcett *et al.*, 2004 Systematic generation of high-resolution deletion coverage of the Drosophila melanogaster genome. *Nat. Genet.* 36: 288–292.
- Peters, J. M., 2002 The anaphase-promoting complex: proteolysis in mitosis and beyond. *Mol. Cell* 9: 931–943.
- Peters, J. M., 2006 The anaphase promoting complex/cyclosome: a machine designed to destroy. *Nat. Rev. Mol. Cell Biol.* 7: 644–656.
- Pichaud, F., and C. Desplan, 2001 A new visualization approach for identifying mutations that affect differentiation and organization of the Drosophila ommatidia. *Development* 128: 815–826.
- Polevoy, G., H. C. Wei, R. Wong, Z. Szentpetery, Y. J. Kim *et al.*, 2009 Dual roles for the Drosophila PI 4-kinase four wheel drive in localizing Rab11 during cytokinesis. *J. Cell Biol.* 187: 847–858.
- Rawls, A. S., and T. Wolff, 2003 Strabismus requires Flamingo and Prickle function to regulate tissue polarity in the Drosophila eye. *Development* 130: 1877–1887.
- Ryder, E., M. Ashburner, R. Bautista-Llacer, J. Drummond, J. Webster *et al.*, 2007 The DrosDel deletion collection: a Drosophila genomewide chromosomal deficiency resource. *Genetics* 177: 615–629.
- Sahai, E., A. S. Alberts, and R. Treisman, 1998 RhoA effector mutants reveal distinct effector pathways for cytoskeletal reorganization, SRF activation and transformation. *EMBO J.* 17: 1350–1361.
- Seifert, J. R., and M. Mlodzik, 2007 Frizzled/PCP signalling: a conserved mechanism regulating cell polarity and directed motility. *Nat. Rev. Genet.* 8: 126–138.
- Simon, M. A., A. Xu, H. O. Ishikawa, and K. D. Irvine, 2010 Modulation of fat:dachsous binding by the cadherin domain kinase four-jointed. *Curr. Biol.* 20: 811–817.
- Simons, M., and M. Mlodzik, 2008 Planar cell polarity signaling: from fly development to human disease. *Annu. Rev. Genet.* 42: 517–540.
- Simons, M., W. J. Gault, D. Gotthardt, R. Rohatgi, T. J. Klein *et al.*, 2009 Electrochemical cues regulate assembly of the Frizzled/Dishevelled complex at the plasma membrane during planar epithelial polarization. *Nat. Cell Biol.* 11: 286–294.
- Starz-Gaiano, M., N. K. Cho, A. Forbes, and R. Lehmann, 2001 Spatially restricted activity of a Drosophila lipid phosphatase guides migrating germ cells. *Development* 128: 983–991.
- Strutt, D., 2003 Frizzled signalling and cell polarisation in Drosophila and vertebrates. *Development* 130: 4501–4513.
- Strutt, D., and H. Strutt, 2007 Differential activities of the core planar polarity proteins during Drosophila wing patterning. *Dev. Biol.* 302: 181–194.
- Strutt, D. I., U. Weber, and M. Mlodzik, 1997 The role of RhoA in tissue polarity and Frizzled signalling. *Nature* 387: 292–295.
- Strutt, H., and D. Strutt, 1999 Polarity determination in the Drosophila eye. *Curr. Opin. Genet. Dev.* 9: 442–446.
- Strutt, H., and D. Strutt, 2003 EGF signaling and ommatidial rotation in the Drosophila eye. *Curr. Biol.* 13: 1451–1457.
- Strutt, H., and D. Strutt, 2008 Differential stability of flamingo protein complexes underlies the establishment of planar polarity. *Curr. Biol.* 18: 1555–1564.
- Strutt, H., and D. Strutt, 2009 Asymmetric localisation of planar polarity proteins: mechanisms and consequences. *Semin. Cell Dev. Biol.* 20: 957–963.
- Strutt, H., M. A. Price, and D. Strutt, 2006 Planar polarity is positively regulated by casein kinase Iepsilon in Drosophila. *Curr. Biol.* 16: 1329–1336.
- Tomlinson, A., and D. F. Ready, 1987 Cell fate in the *Drosophila* Ommatidium. *Dev. Biol.* 123: 264–275.
- Tomlinson, A., and G. Struhl, 1999 Decoding vectorial information from a gradient: sequential roles of the receptors Frizzled and Notch in establishing planar polarity in the Drosophila eye. *Development* 126: 5725–5738.
- Tree, D. R., J. M. Shulman, R. Rousset, M. P. Scott, D. Gubb *et al.*, 2002 Prickle mediates feedback amplification to generate asymmetric planar cell polarity signaling. *Cell* 109: 371–381.
- Usui, T., Y. Shima, Y. Shimada, S. Hirano, R. W. Burgess *et al.*, 1999 Flamingo, a seven-pass transmembrane cadherin, regulates planar cell polarity under the control of Frizzled. *Cell* 98: 585–595.
- Wallingford, J. B., 2006 Planar cell polarity, ciliogenesis and neural tube defects. *Hum. Mol. Genet.* 15(Spec No 2): R227–R234.

- Wallingford, J. B., and R. Habas, 2005 The developmental biology of Dishevelled: an enigmatic protein governing cell fate and cell polarity. *Development* 132: 4421–4436.
- Wang, Y., and J. Nathans, 2007 Tissue/planar cell polarity in vertebrates: new insights and new questions. *Development* 134: 647–658.
- Weber, U., V. Siegel, and M. Mlodzik, 1995 *pipsqueak* encodes a novel nuclear protein required downstream of *seven-up* for the development of photoreceptors R3 and R4. *EMBO J.* 14: 6247–6257.
- Weber, U., C. Eroglu, and M. Mlodzik, 2003 Phospholipid membrane composition affects EGF receptor and Notch signaling through effects on endocytosis during *Drosophila* development. *Dev. Cell* 5: 559–570.
- Weber, U., C. Pataki, J. Mihaly, and M. Mlodzik, 2008 Combinatorial signaling by the Frizzled/PCP and Egfr pathways during planar cell polarity establishment in the *Drosophila* eye. *Dev. Biol.* 316: 110–123.
- Winter, C. G., B. Wang, A. Ballew, A. Royou, R. Karess *et al.*, 2001 *Drosophila* Rho-associated kinase (Drok) links Frizzled-mediated planar cell polarity signaling to the actin cytoskeleton. *Cell* 105: 81–91.
- Wu, J., and M. Mlodzik, 2009 A quest for the mechanism regulating global planar cell polarity of tissues. *Trends Cell Biol.* 19: 295–305.
- Wu, J., T. J. Klein, and M. Mlodzik, 2004 Subcellular localization of frizzled receptors, mediated by their cytoplasmic tails, regulates signaling pathway specificity. *PLoS Biol.* 2: 1004–1014.
- Wu, J., A. Jenny, I. Mirkovic, and M. Mlodzik, 2008 Frizzled-Dish-evelled signaling specificity outcome can be modulated by Diego in *Drosophila*. *Mech. Dev.* 125: 30–42.
- Zeng, X., K. Tamai, B. Doble, S. Li, H. Huang *et al.*, 2005 A dual-kinase mechanism for Wnt co-receptor phosphorylation and activation. *Nature* 438: 873–877.

Communicating editor: T. Schupbach

GENETICS

Supporting Information

<http://www.genetics.org/content/suppl/2012/03/05/genetics.111.137190.DC1>

Novel Regulators of Planar Cell Polarity: A Genetic Analysis in *Drosophila*

Ursula Weber, William J. Gault, Patricio Olguin, Ekaterina Serysheva, and Marek Mlodzik

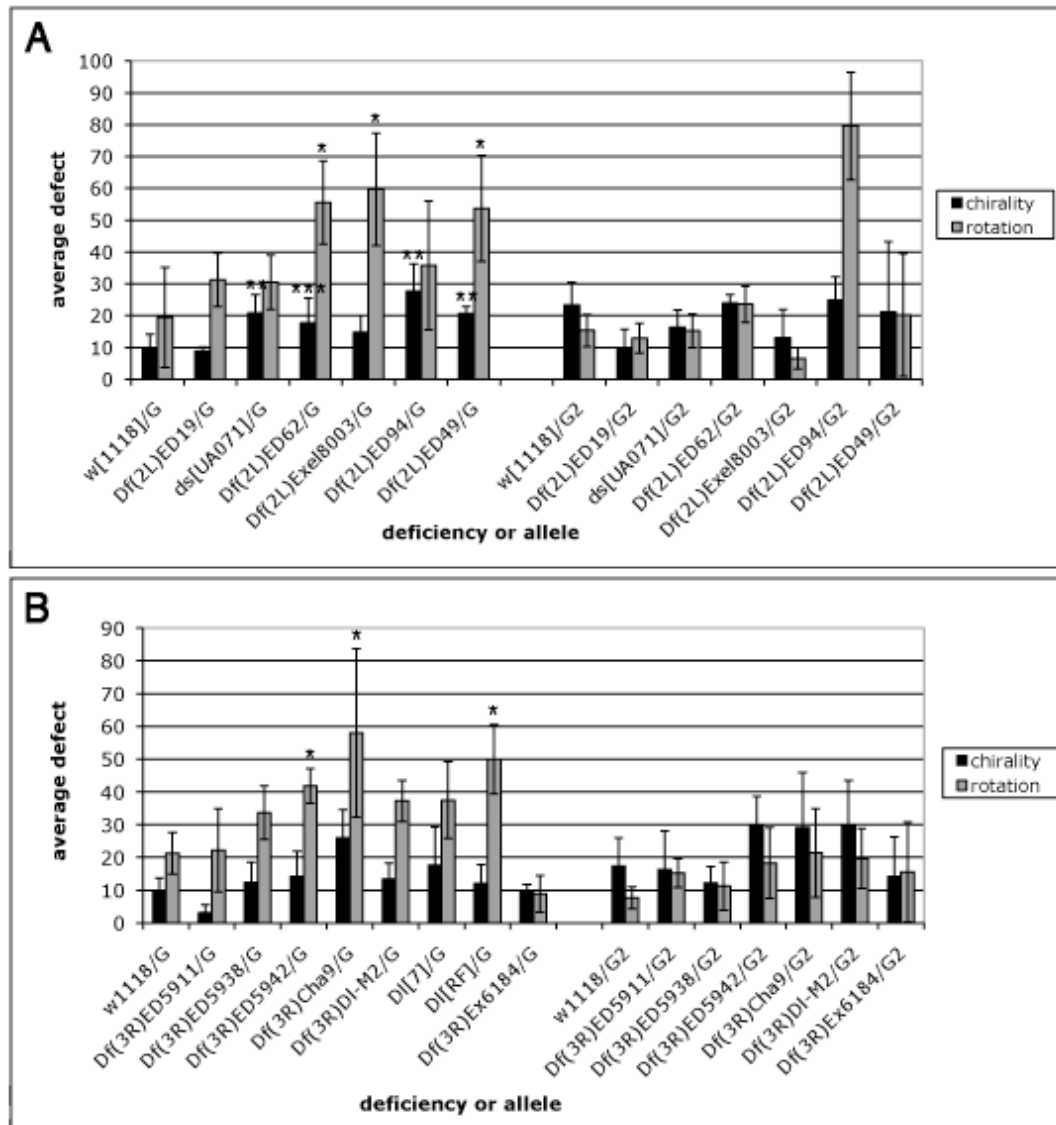


Figure S1 Two interacting DrosDel deficiencies identified in the initial screen covered two known factors, *ds* and *DI*, acting in parallel to or downstream of the Fz/PCP signaling pathway. Graphs show average rotation and chirality defects as determined by the *Rh1-GFP* assay for indicated genotypes for both *sev-Gal4, UAS-dgo* (G) and *sev-Gal4, UAS-pk* (G2). (A) *Df(2R)ED62*, subdividing deficiencies *Df(2R)ED49* and *Df(2R)Exel8003* enhanced rotation defects of *sev-Gal4, UAS-dgo* significantly (*= $P < 0.03$). *Notchless* (*Nle*) might be the candidate gene responsible for that interaction. Subdividing deficiencies *Df(2R)ED49*, *Df(2R)ED94* and *ds^{UA071}* enhanced chirality defects of *sev-Gal4, UAS-dgo* significantly (**= $P < 0.02$), confirming the initial chirality interaction (**= $P < 0.1$) and identifying *dachsous* (*ds*) as the gene responsible for it. No effects were seen with *sev-Gal4, UAS-pk*. *Df(2R)ED94* enhanced rotation defects of *sev-Gal4, UAS-pk*. (B) *Df(3R)ED5942*, subdividing deficiencies *Df(3R)Cha9* and *DI^{RF}* enhanced rotation defects of *sev-Gal4, UAS-dgo* significantly (*= $P < 0.1$), confirming the initial interaction and identifying *Delta* (*DI*) as the gene responsible for it. Deficiency *Df(3R)Cha9* also enhanced chirality defects of *sev-Gal4, UAS-dgo*. 4 eyes were analyzed each and 90-150 ommatidia were evaluated per genotype.

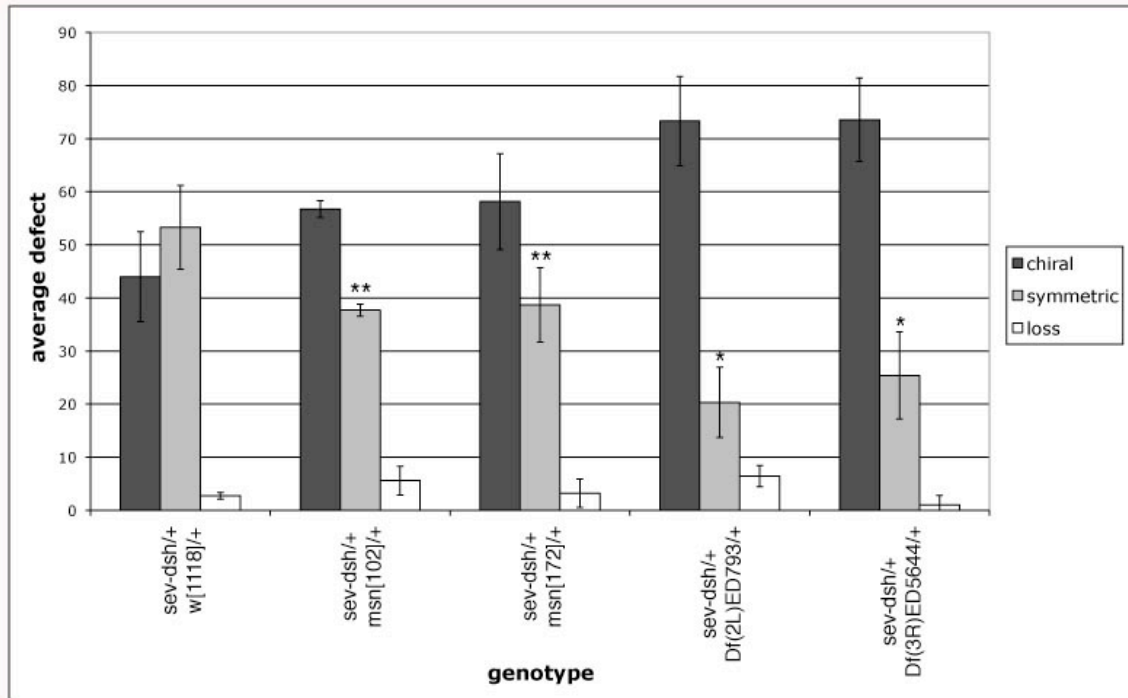


Figure S2 Graph summarizing suppression of *sev-dsh* by two DrosDel deficiencies. Eye sections of 4 eyes were analyzed for ommatidial chirality of indicated genotypes. *Df(2L)ED793* and *Df(3R)ED5644* significantly suppressed *sev-dsh* induced PCP defects of symmetrical photoreceptor arrangement (*= $P < 0.003$). For comparison, the strength of suppression by *misshapen* (*msn*), an established downstream effector of Fz/Dsh signaling in the eye, is shown (**= $P < 0.03$) (Paricio et al. 1999). 2-3 eyes and 200-350 ommatidia were evaluated per genotype.

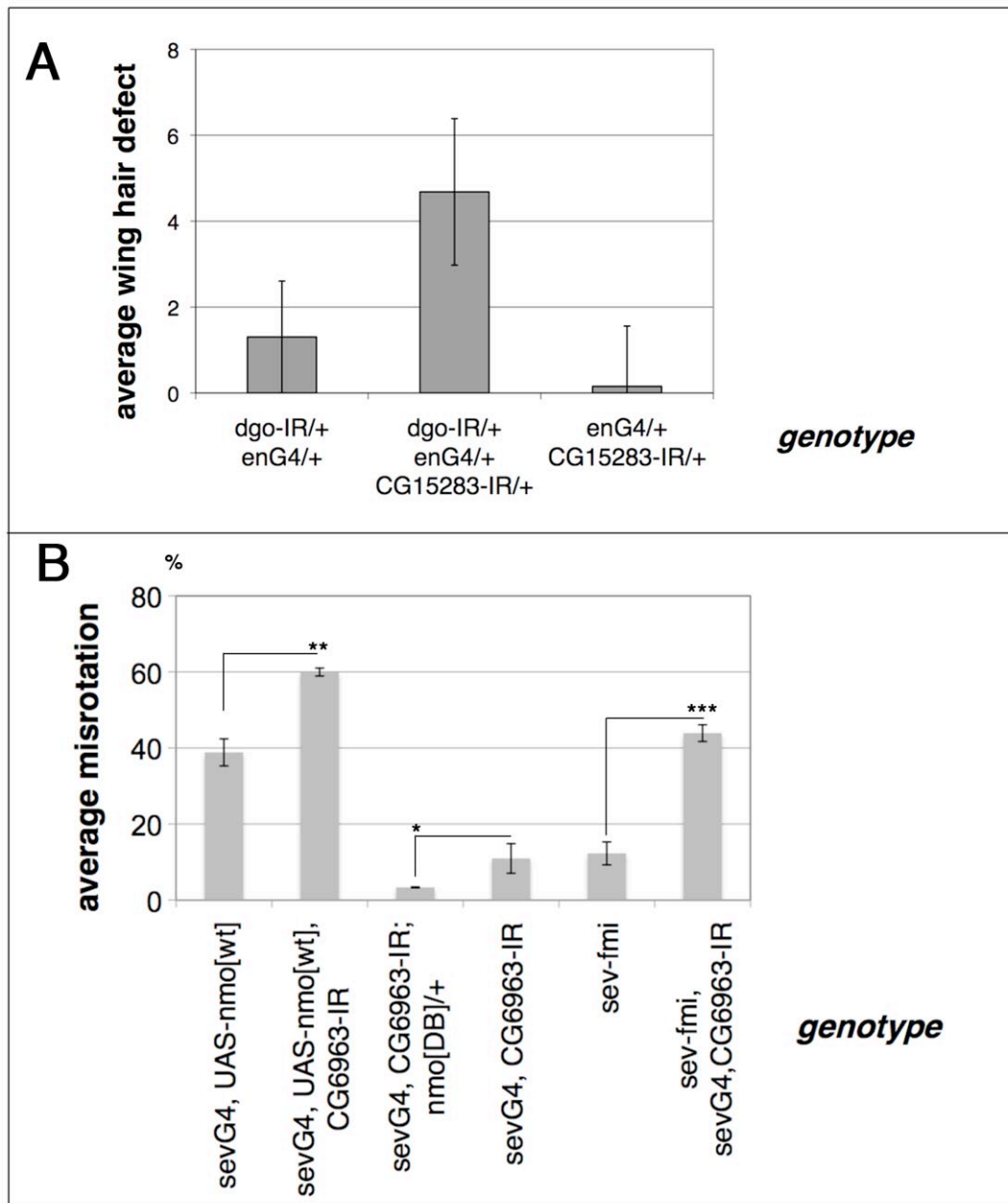


Figure S3 (A) Independent assay confirming *dgo* and *CG15283* loss-of-function interaction. Graph shows average wing hair defects as observed in *en-GAL4*, *UAS-dgo-IR* and enhancement by *CG15283-IR* knockdown. 20 misoriented wing hairs at 45-180 degrees compared to wild-type were recorded as a value of 1 and n was 24-26 wings analyzed for each genotype. (B) Quantification of the rotation defects associated with the *sevGAL4*, *UAS-Nmo*, *CG6963-IR* and *sev-Stan/Fmi* genotypes. Note that *CG6963/CK1g* knock down enhances *Nmo* GOF rotation defects, whereas *nmo*+/+ suppresses the *CG6963-IR* defects, indicating an antagonistic relationship between these genes. In addition, rotation defects associated with *sev-Fmi/Stan* is enhanced by *CG6963-IR* knock down. P values are * <0.03 , ** <0.001 , and *** <0.0001 , with the number of ommatidia analyzed being $n=422-633$ in 3 eyes for each genotype.

Table S1 DrosDel deficiencies, which showed no dominant external eye or wing modification of *sev-GAL4*, *UAS-dgo* and *sev-GAL4*, *UAS-pk* phenotype.

Df(1)ED404	Df(1)ED409	Df(1)ED6574	Df(1)ED411
Df(1)ED6630	Df(1)ED6712	Df(1)ED6802	Df(1)ED418
Df(1)ED6829	Df(1)ED6991	Df(1)ED7005	Df(1)ED429
Df(1)ED7067	Df(1)ED7153	Df(1)ED7217	Df(1)ED7229
Df(1)ED7294	Df(1)ED7355	Df(1)ED7413	Df(1)ED6906
Df(1)ED7664	Df(1)ED6849	Df(2L)ED2809	Df(2L)ED5878
Df(2L)ED19	Df(2L)ED87	Df(2L)ED94	Df(2L)ED108
Df(2L)ED125	Df(2L)ED123	Df(2L)ED136	Df(2L)ED247
Df(2L)ED284	Df(2L)ED508	Df(2L)ED647	Df(2L)ED678
Df(2L)ED690	Df(2L)ED701	Df(2L)ED737	Df(2L)ED761
Df(2L)ED778	Df(2L)ED3	Df(2L)ED1050	Df(2L)ED1102
Df(2L)ED1109	Df(2L)ED1158	Df(2L)ED1165	Df(2L)ED1186
Df(2L)ED1226	Df(2L)ED1231	Df(2L)ED1303	Df(2L)ED1384
Df(2L)ED1473	Df(2R)ED1484	Df(2R)ED1612	Df(2R)ED1735
Df(2R)ED2155	Df(2R)ED2219	Df(2R)ED9045	Df(2R)ED2354
Df(2R)ED2426	Df(2R)ED2436	Df(2R)ED1	Df(2R)ED3610
Df(2R)ED3923	Df(2R)ED4061	Df(2R)ED4071	Df(2R)Exel6061
Df(2R)ED1770	Df(2R)ED2098	Df(3L)ED4079	Df(3L)ED4256
Df(3L)ED4287	Df(3L)ED4288	Df(3L)ED4341	Df(3L)ED4342
Df(3L)ED210	Df(3L)ED211	Df(3L)ED4408	Df(3L)ED4421
Df(3L)ED4457	Df(3L)ED4475	Df(3L)ED215	Df(3L)ED4486
Df(3L)ED217	Df(3L)ED218	Df(3L)ED223	Df(3L)ED4674
Df(3L)ED4685	Df(3L)ED4710	Df(3L)ED224	Df(3L)ED225
Df(3L)ED4782	Df(3L)ED4786	Df(3L)ED228	Df(3L)ED4799
Df(3L)ED4978	Df(3L)ED231	Df(3R)ED4710	Df(3R)ED5138
Df(3R)ED5147	Df(3R)ED5156	Df(3R)ED5177	Df(3R)ED5196
Df(3R)ED5230	Df(3R)ED5343	Df(3R)ED5429	Df(3R)ED5591
Df(3R)ED5610	Df(3R)ED5642	Df(3R)ED10642	Df(3R)ED5780
Df(3R)ED2	Df(3R)ED5911	Df(3R)ED6025	Df(3R)ED10809
Df(3R)ED10820	Df(3R)ED6093	Df(3R)ED6103	Df(3R)ED6187
Df(3R)ED6235	Df(3R)ED6255	Df(3R)ED6265	Df(3R)ED6310
Df(3R)ED6316	Df(3R)ED6332	Df(3R)ED6346	Df(3R)ED5071
Df(4)ED6364	Df(4)ED6369	Df(4)ED6380	Df(4)ED6382
Df(4)ED6384			